FABRICATION OF POLY (LACTIC ACID)/POLY (BUTYLENE ADIPATE-CO-TEREPHTHALATE) CELL SCAFFOLD FOR SOCKET PRESERVATION

KULLAPOP SUTTIAT

**DOCTOR OF PHILOSOPHY
IN BIOMEDICAL ENGINEERING**

**GRADUATE SCHOOL
CHIANG MAI UNIVERSITY
FEBRUARY 2023**

FABRICATION OF POLY (LACTIC ACID)/ POLY (BUTYLENE ADIPATE-CO-TEREPHTHALATE) CELL SCAFFOLD FOR SOCKET PRESERVATION

KULLAPOP SUTTIAT

DOCTOR OF PHILOSOPHY
IN BIOMEDICAL ENGINEERING

GRADUATE SCHOOL
CHIANG MAI UNIVERSITY
FEBRUARY 2023

FABRICATION OF POLY (LACTIC ACID)/POLY (BUTYLENE ADIPATE-CO-TEREPHTHALATE) CELL SCAFFOLD FOR SOCKET PRESERVATION

KULLAPOP SUTTIAT

A THESIS SUBMITTED TO CHIANG MAI UNIVERSITY IN PARTIAL FULFILLMENT OF THE REQUIREMENTS FOR THE DEGREE OF DOCTOR OF PHILOSOPHY IN BIOMEDICAL ENGINEERING

GRADUATE SCHOOL, CHIANG MAI UNIVERSITY FEBRUARY 2023

a

FABRICATION OF POLY (LACTIC ACID)/POLY (BUTYLENE ADIPATE-CO-TEREPHTHALATE) CELL SCAFFOLD FOR SOCKET PRESERVATION

KULLAPOP SUTTIAT

THIS THESIS HAS BEEN APPROVED TO BE A PARTIAL FULFILLMENT
OF THE REQUIREMENTS FOR THE DEGREE OF
DOCTOR OF PHILOSOPHY
IN BIOMEDICAL ENGINEERING

Examination Committee:

…………………………Chairman
(Asst. Prof.Dr. Parkpoom Jarupoom)

…………………………Member
(Assoc.Prof.Dr. Wassanai Wattanutchariya)

…………………………Member
(Assoc.Prof.Dr. Winita Punyodom)

…………………………Member
(Asst.Prof.Dr. Anirut Chaijaruwanich)

…………………………Member
(Dr. Chawan Manaspon)

Advisory Committee:

…………………………Advisor
(Assoc.Prof.Dr.Wassanai Wattanutchariya)

…………………………Co-advisor
(Assoc.Prof.Dr. Winita Punyodom)

…………………………Co-advisor
(Asst.Prof.Dr. Anirut Chaijaruwanich)

20 February 2023
Copyright © by Chiang Mai University

b

To

My beloved family and everyone, who raised a light for me.

ACKNOWLEDGEMENT

This project would not have been possible without the support of many people. Firstly, I would like to express my thanks to my patient and supportive supervisor, Assoc. Prof. Dr. Wassanai Wattanatchariya, who has supported and guided me throughout this research project. Many thanks would also give to my committee members, Assoc. Prof. Dr. Winita Punyodom, Asst. Prof. Dr. Anirut Chaijaruwanich, and Dr. Chawan Manaspon. Your encouragement and feedback have been very important to me.

I would also like to thank Dr. Chawal Manaspon for his excellence cell culture training course. In addition, I would like to thank Dr. Kittiya Thunsiri, Dr. Suruk Udomsom, Dr. Pathinan Paengnakorn, and Dr. Phornsawat Baipaywad for their technical assistance throughout my research. I would like to say a special thank you to Biomedical Engineering Institute, Chiang Mai University and all staffs for their generosity and encouragement.

Finally, I would like to acknowledge the faculty of Dentistry, Chiang Mai University, as well as all staff members at the department of Prosthodontics for their supports on my PhD study. I would also like to acknowledge the financial support from the National Research Council of Thailand (NRCT), grant no. 2934737. Most importantly, I would like to thank my family and numerous friends who endured this long process with me, always offering support and love.

<div align="right">Kullapop Suttiat</div>

d

หัวข้อดุษฎีนิพนธ์	การสร้างโครงเลี้ยงเซลล์โพลีแลคติกเอซิด/พอลิบิวทิลีน
	อะดิเพท-โค-เทเรฟทาเลต เพื่อการคงสภาพเบ้าฟัน
ผู้เขียน	นายกุลภพ สุทธิอาจ
ปริญญา	ปรัชญาดุษฎีบัณฑิต (วิศวกรรมชีวการแพทย์)
คณะกรรมการที่ปรึกษา	รศ.ดร. วัสสนัย วรรธนัจฉริยา อาจารย์ที่ปรึกษาหลัก
	รศ. ดร. วินิตา บุญโยดม อาจารย์ที่ปรึกษาร่วม
	ผศ.ดร. อนิรุท ไชยจารุวณิช อาจารย์ที่ปรึกษาร่วม

บทคัดย่อ

การพัฒนาโครงเลี้ยงเซลล์ที่มีลักษณะทางกายภาพและสมบัติทางชีววิทยาที่เหมาะสมสำหรับการฟื้นฟู
เนื้อเยื่อกระดูกเป็นสิ่งท้าทายในงานวิจัยวิศวกรรมเนื้อเยื่อ การศึกษาครั้งนี้มีวัตถุประสงค์เพื่อสร้าง
โครงเลี้ยงเซลล์ชนิดรูพรุนที่ย่อยสลายได้จากพอลิเมอร์ผสม โพลีแลคติกเอซิด/พอลิบิวทิลีน อะดิเพท-
โค-เทเรฟทาเลต เพื่อใช้เติมเบ้าฟันหลังการถอนฟัน ผลการศึกษาลักษณะทางกายภาพ สมบัติทางเคมี
รวมทั้งสมบัติทางชีวภาพต่อเซลล์ออสทีโอบลาสต์ของมนุษย์ (MG-63) แสดงให้เห็นว่า เทคนิคการ
สร้างโครงเลี้ยงเซลล์ด้วยการอัดแก็สและการชะล้างเกลือแอมโมเนียมไบคาร์บอเนต สามารถสร้าง
พรุนแบบเปิด ขนาดเส้นผ่านศูนย์กลาง 10 – 100 นาโนเมตร และ 200- 300 นาโนเมตร ที่เรียงตัวอย่าง
ไม่เป็นระเบียบ กระจายทั่วทั้งชิ้นงาน การศึกษาด้วย SEM, EDX, FTIR, และ XRD ยืนยันการเกิดชั้น
ซึ่งประกอบด้วยพอลิโดปามีน แคลเซียมฟอสเฟตชนิดอสัญฐาน และผลึกไฮดรอกซีอะพาไทต์ บนผิว
ของโครงเลี้ยงเซลล์ หลังการปรับปรุงผิวด้วยพอลิโดปามีนและการสะสมแร่ธาตุโดยการแช่ใน
สารละลายจำลองของเหลวในร่างกายความเข้มเข้น 10 เท่า โครงเลี้ยงเซลล์ที่พัฒนาขึ้นมีลักษณะ
ยืดหยุ่น มีค่าความพรุนเฉลี่ย 84.17±1.29%, ค่าเฉลี่ยมุมสัมผัส 45.7±5.9 องศา และ อัตราการสลายตัว
7.63±2.56% โครงเลี้ยงเซลล์ไม่แสดงความเป็นพิษต่อเซลล์ออสทีโอบาล์สของมนุษย์ และมีสมบัติชัก
นำการสร้างกระดูก การศึกษาครั้งนี้แสดงให้เห็นถึงความเป็นไปได้ในการประยุกต์ใช้โครงเลี้ยงเซลล์
ชนิดรูพรุนที่สร้างจากพอลิเมอร์ผสม โพลีแลคติกเอซิด/พอลิบิวทิลีน อะดิเพท-โค-เทเรฟทาเลต และ
ได้รับการปรับสภาพผิวด้วยพอลิโดปามีนและการสะสมแร่ธาตุ เป็นวัสดุทางเลือกเพื่อการฟื้นฟู
กระดูกเบ้ารากฟัน สำหรับคงเค้ารูปของกระดูกเบ้าฟันหลังการถอนฟัน

Dissertation Title   Fabrication of Poly(lactic acid)/Poly(butylene adipate-co-terephthalate) Cell Scaffold for Socket Preservation

Author   Mr. Kullapop Suttiat

Degree   Doctor of Philosophy (Biomedical Engineering)

Advisory Committee   Assoc. Prof. Dr. Wassanai Wattanutchariya Advisor
    Assoc. Prof. Dr. Winita Punyodom   Co-advisor
    Asst. Prof. Dr. Anirut Chaijaruwanich   Co-advisor

ABSTRACT

The development of scaffold with optimal physiological and biological characteristics is crucial in tissue engineering. This study aims to fabricate the biodegradable scaffold with highly porous architecture and osteogenic potential using the poly(lactic)/poly(butylene adipate-co-terephthalate) (PLA/PBAT) blend for applying as the socket filling material following natural tooth removal. The evenly formation of less ordered opened porous cells with different diameters ranged from 10-100 µm and 200-300 µm as well as the presence of the well interconnected network that positively influenced on bone regenerative process were resulted through the gas foaming/ammonium bicarbonate particulate leaching technique. The analysis by SEM, EDX, FTIR, and XRD confirmed the deposition of biocomposites composed of the polydopamine (PDA), amorphous calcium phosphate (ACP), and hydroxyapatite (HA) crystals following the PDA assisted-biomineralization by soaking in ten times concentrated simulated body fluid (10x-SBF) solution. The scaffold showed the compressible property with the total porosity of 84.17±1.29%, the low contact angle of 45.7±5.9 degree, and the material degradation rate of 7.63±2.56%. The biological evaluations by MTT assay and Alizarin Red S (ARS) staining confirmed the biocompatibility and osteogenic potential of the developing scaffold toward the human osteoblast-like cell (MG-63). Overall, the porous PLA/PBAT scaffold with PDA-assisted biomineralization exhibits the promising potential as the alternative porous biomaterial for tooth socket preservation following natural tooth loss.

CONTENTS

LIST OF FIGURES

LIST OF FIGURES (continued)

Page

i

LIST OF FIGURES (continued)

LIST OF ABBREVIATIONS

ΔHm	enthalpy of melting
ANOVA	analysis of variance
ARS	Alizarin Red S Staining
CaP	calcium phosphate
DA	dopamine
dECM	demineralized extracellular matrix
DMEM	Dulbecco's modified Eagle medium
DMSO	dimethyl sulfoxide
DSC	differential scanning calorimeter
ECM	extra cellular matrix
EDX	energy-dispersive X-ray analysis
FTIR	Fourier transform infrared spectroscopy
HA	hydroxyapatite
MTT	3-[4,5-dimethylthiazol-2-yl]-2,5 diphenyl tetrazolium bromide)
OD	optical density

LIST OF ABBRIVIATIONS (continued)

PBAT	poly(butylene adipate-co-terephthalate)
PBS	phosphate buffer solution
PDA	polydopamine
PEG	poly(ethylene glycol)
PLA	poly(lactic acid)
SBF	simulated body fluid
SEM	scanning electron microscope
T_g	glass transitional temperature
T_m	melting temperature
XRD	X-ray diffraction

ข้อความแห่งการริเริ่ม

1) ดุษฎีนิพนธ์นี้ได้เสนอกระบวนการเตรียมโครงเลี้ยงเซลล์ที่มีรูพรุนเชื่อมต่อกันและมีสมบัติ
ทางชีวภาพต่อเซลล์ออสทีโอบลาสต์ของมนุษย์ (MG-63) จากพอลิเมอร์ผสมโพลีแลคติกเอ
ซิด/พอลิบิวทิลีน อะดิเพท-โค-เทเรฟทาเลต เพื่อใช้เป็นวัสดุชีวภาพสำหรับอุดในเบ้าฟัน
สำหรับคงเค้ารูปเดิมของกระดูกในบริเวณดังกล่าวหลังการถอนซี่ฟันธรรมชาติ โครงเลี้ยง
เซลล์ชนิดรูพรุนต่อเนื่องที่พัฒนาขึ้นด้วยเทคนิคการอัดแก๊สและการชะล้างเกลือแอมโมเนียม
ไบคาร์บอเนต ร่วมกับการปรับปรุงผิวด้วยพอลิโดปามีนและการสะสมแร่ธาตุโดยการแช่ใน
สารละลายจำลองของเหลวในร่างกายความเข้มข้น 10 เท่า มีลักษณะทางกายภาพและสมบัติ
ทางชีวภาพที่เหมาะสมสำหรับการนำมาประยุกต์ใช้ในกระบวนการฟื้นฟูกระดูก

2) โครงเลี้ยงเซลล์ชนิดรูพรุนโพลีแลคติกเอซิด/พอลิบิวทิลีน อะดิเพท-โค-เทเรฟทาเลตที่ได้รับ
การปรับสภาพพื้นผิวด้วยพอลิโดปามีนร่วมกับการสะสมแร่ธาตุโดยการแช่ในสารละลาย
จำลองของเหลวในร่างกายความเข้มข้น 10 เท่า แสดงลักษณะทางกายภาพและสมบัติทางเคมี
ที่เหมาะสมต่อการเติบโตและพัฒนาเซลล์ออสทีโอบลาสต์ของมนุษย์ กล่าวคือ มีรูพรุนที่
เชื่อมต่อกันทั่วทั้งชิ้นงาน รูพรุนแบบเปิดภายในชิ้นงานมีขนาดเส้นผ่านศูนย์กลางอยู่ในช่วงที่
เหมาะสมสำหรับการเติบโตและพัฒนาของเซลล์กระดูก การสะสมของแคลเซียม ฟอสเฟต
หลังการปรับสภาพผิวส่งผลให้พื้นผิวของรูพรุนที่มีความขรุขระในระดับนาโน ทำให้เกิด
สภาพแวดล้อมในระดับจุลภาพที่ส่งผลในเชิงบวกต่อการเติบโตและพัฒนของเซลล์กระดูก
รวมไปถึงกระบวนการฟื้นฟูของกระดูก นอกจากนั้นการปรับสภาพพื้นผิวยังส่งผลให้โครง
เลี้ยงเซลล์มีความชอบน้ำเพิ่มขึ้น อีกทั้งการสะสมของชั้นคอมพอสิตทางชีวภาพ ซึ่ง
ประกอบด้วยพอลิโดปามีน แคลเซียมฟอสเฟตชนิดอสัญฐาน และผลึกไฮดรอกซีอะพาไทต์
บนผิวของโครงเลี้ยงเซลล์ ยังทำให้ผิวของโครงเลี้ยงเซลล์มีคุณสมบัติกระตุ้นการตอบสนอง
ทางชีวภาพต่อเซลล์ออสทีโอบลาสต์ของมนุษย์และกระบวนการฟื้นฟูของกระดูก

3) การประยุกต์ใช้เทคนิกการอัดแก็สและการชะล้างเกลือแอมโมเนียมไบคาร์บอเนต ร่วมกับ
การปรับปรุงผิวด้วยพอลิโดปามีนและการสะสมแร่ธาตุโดยการแช่ในสารละลายจำลอง
ของเหลวในร่างกายความเข้มเข้น 10 เท่า เป็นเทคนิกสำหรับสร้างโครงเลี้ยงเซลล์ชนิดรูพรุน
ที่มีความต่อเนื่อง และมีสมบัติทางชีวภาพที่เหมาะสำหรับการเติบโตของเซลล์ออสทีโอบ
ลาสต์ของมนุษย์ ที่มีราคาถูก และไม่ซับซ้อน สามารถประยุกต์ใช้ได้กับวัสดุหลากหลายชนิด
รวมถึงวัสดุที่มีโครงสร้างซับซ้อน และมีความเป็นไปได้ที่จะนำไปประยุกต์ใช้ในทางคลินิก

n

STATEMENTS OF ORIGINALITY

1) This thesis proposes the procedure for preparing the porous PLA/PBAT scaffold with well interconnected network and simultaneously provides the bioactive property and osteogenic potential toward the human osteoblast like cell (MG-63) for using as the tooth socket filling material to preserve the original alveolar bone contour following the natural tooth loss. The newly developed PLA/PBAT porous scaffold prepared through the combination of the gas foaming/ ammonium bicarbonate leaching technique for porous scaffold preparation and PDA-assisted biomineralization in 10x-SBF solution for osteogenic surface improvement exhibited the suitable physical and biological properties for improving the bone regenerative process.

2) The surface morphology and chemistry of the developed porous PLA/PBAT scaffold with PDA-assisted biomineralization provides the microenvironment that provides a positive effect on the bone cell bioactivity as well as bone regenerative process. The various diameters of the opened porous cells and the high porosity, the formation of the roughness in nano-level following the surface modification, the improvement on material hydrophilicity, the formation of bioactive composite that comprised of PDA, amorphous calcium phosphate, and hydroxy apatite crystals are positively influenced on the osteoblast cell behaviors and bone regenerative mechanism.

3) This technique is simple, inexpensive, and effective to fabricate the polymeric scaffold with high porous structure and osteogenic potential. It does not need a special equipment or conditions. It can perform in almost surfaces at the atmospheric pressure under mild and less harmful fabricating conditions. This advantage made it is possible for using in clinical scenario.

CHAPTER 1

Introduction

1.1 Histological Background

Generally, the destruction or degeneration of tissue due to the disease, injury and trauma requires the treatments to facilitate the healing, replacement or regeneration of the defective tissues or structures. The conventional treatment paradigm focuses on removing the defective tissues or organs then replaces with the sound tissues or organs to restore the physical morphology and/or functions of the pathological structures. According to this treatment paradigm, the grafting material are generally collected from the patient own tissue (autograft), the animals (xenograft), or another human (allograft).

This approach provides the good clinical outcome. Nevertheless, they have the major drawbacks that significantly limited the application in some scenarios. The expensive and complicated surgical procedures, post operative pain, the limitations on the anatomical and amount of the donor site as well as the patient morbidity due to the wound infection, hematoma or tissue swelling are the major limitations for tissue substitution with the autograft materials. In addition, the tissue replacement by allograft or xenograft also exhibits the serious constraints due to the risks of the patient's immune rejection including the possibility of infection or disease transmission from the donor to the recipient.

Alternatively, the tissue engineering concept which aim to regenerate the destructive tissues or structures, instead of replacing, has been interested as the new paradigm for restoring the deteriorated tissues. The regeneration of the damaged structures by the patient's own tissue is the distinctive character of this approach. By this concept, the poor biocompatibility of substitute materials, the low bio-functionality as well as the risks of the adverse effects caused from the immune rejection or disease transmission have been solved. Due to its outstanding advantages, tissue engineering is often considered as the

1

promising and alternative treatment strategy for restoring the destructive structures in the modern world of medicine and dentistry.

The tissue repairing by tissue engineering concept bases on three main factors, cells, scaffold, and bio-signals. All of these three factors play a major role on the tissue regenerative process. The patient's own cells are necessary for the new tissue matrix formation, while the porous scaffold gives the temporary support for the precursor cells to adhere, proliferate, and differentiate to the target tissues or organs. The biological mediator plays a major role on facilitating and enhancing precursor cells to regenerate new tissue.

Among these three main factors, the tissue scaffold has been extensively researched for the specific purposes in the tissue regenerative medicine. Most of the previous articles focused on the development of the novel porous 3D scaffolds with an appropriate cellular microenvironment to fulfill the basic requirements for enhancing the patients 'cells bioactivities and tissue regeneration process. However, the development of synthetic cell scaffolds to function as the artificial extracellular matrix which have proper microarchitectures, mechanically stability, biocompatibility, and biodegradable as well as bioactive properties to each individual cell type still be a major challenge in tissue engineering research. This requirement highlights the need for novel approaches to overcome the persisting challenges.

Nowadays, the attentions on applying the tissue engineering as the alternative modality to restore the defective tissues has been dramatically increased in both medical and dental scenarios. In dentistry, the concept of tissue regeneration has normally been applied in various types of bone reconstructive procedures including the tooth socket preservation technique. The clinical success in reducing the alveolar bone contour alteration following the natural tooth loss by the placement of the synthetic biomaterials into the extraction tooth socket as the scaffold for alveolar bone cells has been addressed in the previous clinical investigations. This finding evidences the increasing of the effort on adapting the concept of tissue regeneration into the routine dental treatment modalities. Moreover, it also indicates that the tissue engineering could be concerned as the treatment approach for the future.

2

1.2 Objectives

The development of tissue scaffold which classified as one of the three main fundamental factors of tissue engineering has been dramatically mentioned in the previous articles. The advance on the materials science and biological chemistry are the significant factors that provoked the extensive studies on development of the synthetic tissue scaffold for tissue regenerative purpose. Most of studies focus on preparing the three-dimensional porous specimens with the specific mechanical and bioactive properties according to the specific clinical application. For this reason, the present study aims to

1.2.1   fabricate the three-dimensional opened porous PLA/PBAT scaffold with well interconnected network and osteogenic property to human osteoblast-like cell (MG-63).

1.2.2   characterize the scaffold morphology, material properties, *in vitro* degradation rate, and the biological responses to human osteoblast-like cells (MG-63).

1.2.3   evaluate the possibility on applying the developing scaffold as the alternative tooth socket filling material for tooth socket preservation technique.

1.3 Principal, Theory and Rationale

Natural tooth extraction is one of the most common dental practices in daily life. This treatment modality indicates when a natural tooth is in a non-restorable condition or has a poor prognosis in a long-term period. Commonly, the dental caries and periodontal diseases are the main reasons for tooth extraction.

Once the natural tooth has taken out, the histological events of the healing process is initiate. It begins with the formation of clot inside the extraction socket and end up with the formation of new bone inside the extraction socket with the epithelization on top (Amler, 1969; Cardaropoli et al., 2003). The formation of the uneven bone contour at tooth extracted site is the common consequence following this process. In most cases, alveolar bone of the socket undergoes a reduction in width of around 50% within the first year (Araújo & Lindhe, 2005). However, the individual difference of bone alteration

3

following tooth extraction was mentioned in the previous article (Atwood, 1963). Within the same jaw, the greater amount of the alveolar resorption is observed on the buccal rather than the palatal or lingual side. Comparing between upper and lower jaws, the remarkable bone resorption is found on maxilla than the mandible (Araújo & Lindhe, 2005; Lekovic et al., 1998).

For patients with totally loss of their natural teeth, the continuous ridge resorption following the tooth loss may lead to the inverse relationship between upper and lower jaw as the inverse resorbed direction (Araújo & Lindhe, 2005; Pietrokovski & Massler, 1967). This bony change may result in the protruding chin that usually mentioned as the classical appearance of the denture wearer (Lekovic et al., 1998; Pietrokovski & Massler, 1967).

In case of the partial tooth loss, the uneven edentulous ridge contour on buccal side of alveolar ridge and the reduction of the alveolar bone height are usually observed. The data from radiographic studies exhibited the largely loss of alveolar ridge height within the first 90 days following tooth loss. After six months following the tooth extraction, the horizontal and vertical bone loss are expected as 29% to 63% and 11% to 22% respectively (Fickl et al., 2008; Schropp et al., 2003).

The bone contour alteration following tooth extraction may lead to two main clinical challenging situations. First, it may significantly compromise the esthetic outcomes of the fixed dental prostheses especially at the anterior part of the jaw. Second, it can make the challenge in dental implant placement due to the inadequate bone quantity at the implant placement site (Farmer & Darby, 2014; Masaki et al., 2015) as presented in Figure 1.1. Therefore, the clinical procedure for preventing the alveolar ridge contour alteration following tooth extraction is concerned as one of the challenged topics in the modern dentistry (Brandam et al., 2015; Farmer & Darby, 2014; Papadimitriou et al., 2014).
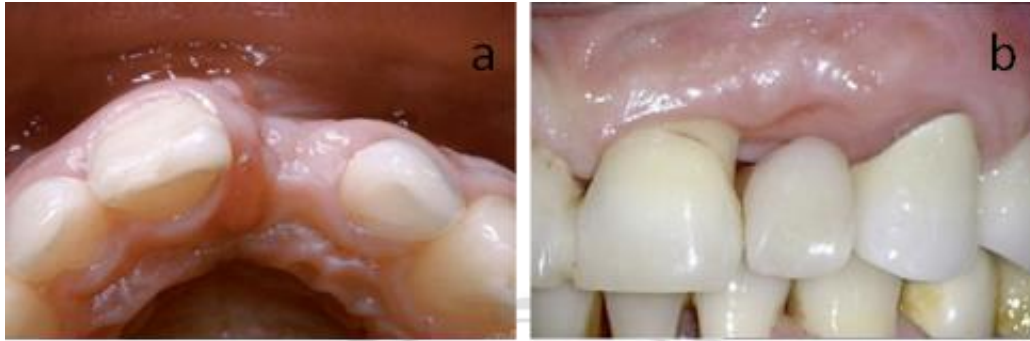
Figure 1.1. The compromised in esthetic of dental prostheses due to the alteration of alveolar ridge volume following natural tooth extraction. The concavity on buccal side of alveolar ridge following the natural tooth removal (a). The reduction of alveolar bone height at the extracted area resulted in uneven ridge height in edentulous area (b).

Various techniques have been introduced to correct or prevent the bone resorption following the natural tooth loss. Ridge preservation technique is one of the effective clinical procedures for controlling or minimizing the dimensional change of alveolar ridge following natural tooth loss (Lekovic et al., 1998; Lekovic et al., 1997). This approach involves the filling of the extraction socket with appropriate grafting materials to form a template or framework during the bone regenerative process at the tooth extracted sites (Artzi & Nemcovsky, 1998; Christensen, 1996). Briefly, the socket preservation technique starts with atraumatic extraction to preserve the thin buccal and palatal bone wall of the extracted socket. Then, the socket is filled with the appropriate scaffold as a framework for bone precursor cells to encourage the newly bone formation process (Figure 1.2).

Figure 1.2. The clinical procedures for socket preservation technique. Non-traumatic tooth extraction is performed to preserve the buccal and palatal bone plates (a). The appropriate biomaterial is placed into the socket to enhance bone regenerating process (b). The example of commercially available porous scaffold for tooth socket preservation (c).

Since the introduction of this technique, many attempts on developing the appropriate biomaterials as the socket grafting materials have been addressed. The conventional bone substitute materials, including autogenous, allogenous and xenograft, have been considered as gold standard for decades (Amini et al., 2012). However, the inherent disadvantages and the adverse effects in histological level of conventional bone grafting materials are the major drawbacks that limited the clinical application (Becker et al., 1996; Froum et al., 2002; Heberer et al., 2008). This problem challenges the researcher to develop the new biomaterials which provide the suitable properties over the conventional bone graft materials.

6

The application of the autologous bone graft normally requires the surgical operations for bone harvesting from the donor sites that may cause the adverse effects to the patient including the morbidity, uncomfortable feeling, and post-operative pain. Furthermore, the limitations on the size and amount of bone that can be collected from the patient without interfering the normal functions are the significant aspects that needed to be concerned. Furthermore, the risk on the immune rejection or disease transmission cause from the allogenic or xenogenic bone grafting placement are the serious complications that significantly restricted the clinical application (Draenert et al., 2016; Reichert et al., 2011). To overcome these inherent drawbacks, the synthetics scaffolds have been developed and recommended as an alternative material.

The cell supported framework, known as a scaffold, is one of the three major key factors of tissue engineering. It plays a crucial role on the success of the tissue regenerative approach (Hutmacher et al., 2007). For bone scaffold, the presence of the microarchitectures which mimicking the natural bone extracellular matrix (ECM) structure is concerned as one of the fundamental requirements that significantly influence on bone formative process. This microenvironment facilitates the bone progenitor cells to adhere and differentiate to bone cells that directly influences to the bone cells regulation and new bone forming process.

Moreover, bone scaffold also requires the simulation of chemical compositions as well as the bioactive property of native bone (Langer & Vacanti, 1993). However, the development of the synthetic biomaterials that fulfilled all basic requirements for bone tissue engineering has not yet been encountered. This aspect is still the one of the ultimate challenges in tissue engineering field (Mercado-Pagan et al., 2015).

As the extensive growing of the attention on applying the biodegradable polymers as the alternative to the conventional materials in last few decades, the applications of various biodegradable polymers on various purposes including the medical and dental treatments have been noticed (Kohane & Langer, 2008; Song et al., 2018). However, only the several types of synthetic aliphatic polymer have been focused and recommended as the material for bone scaffold fabrication. The poly (lactic acid) (PLA) which approved by USA Food and Drug Administration (FDA) as the versatile biopolymer for medical application is

7

one of the promising polymers suitable for applying in bone regenerative purpose. The excellence biocompatibility and the controlled biodegradation of PLA are main advantages that attracted the interesting of researchers to use this polymer as a based material for generating the imitate extracellular matrix for tissue regenerative application (Liu et al., 2020). However, the insufficient mechanical properties including the poor cell recognition sites, lack of the osteoinductive property and low hydrophilic character are the significant inherent disadvantages that limited the clinical applications of this polymer (DeStefano et al., 2020).

Several materials modification techniques such as the copolymerization, plasticization and blending with various biodegradable polymers have been suggested to improve and engineer the mechanical properties of the virgin matrix. The excellent physio-chemical and mechanical properties particularly the material toughness has been reported in the blend of PLA and biodegradable polybutylene adipate-co-terephthalate (PBAT) (Farah et al., 2016; Ferreira et al., 2019). For bioactive modification, the development of composite material is proposed to overcome the inherent disadvantages of pure polymer (Idaszek et al., 2013). The combination of synthetic polymer and bioactive components is the simple and effective strategies in material science to improve the bioactivity and biocompatibility of the bioinert polymers.

The scaffold with three-dimensional porous architecture and bioactive property plays a major role on preserving the tissue volume, providing the temporary supportive framework for cells, and delivering the bioregulation signals for cell activities. Moreover, the cell infiltration, cell migration, vascularization, the exchange of nutrients and oxygen as well as the removal of the waste products from the recipient site that significantly affected to the success of the tissue regenerative process are major influenced by the sufficient porosity, suitable pore size, and well interconnections inside the scaffold (Limmahakhun et al., 2017). Therefore, the synthetic scaffold properly for bone regeneration should have both the high porosity, appropriated size of opened porous structures, well interconnected networks, and osteogenic property.

For this reason, the present study will focus on developing the scaffold with the interconnected porous microstructures from the biodegradable polymer. The bioactive

8

property and surface morphology of the developing scaffold will be tailored to favor the basic requirements of bone regenerative process. The literature reviews regarding the development of porous scaffold for bone tissue engineering are presented as following.

1.2 Literature review

1.2.1 Bone components

Bone is a heterogeneous bio-composite material which has a highly specialized organic-inorganic compositions and structures. The mineral phase which exhibits a similarity in composition and structure to the synthetic hydroxyapatite (HA) is embedded in an organic extracellular matrix (ECM). However, the presence of the ionic substitutions such as CO_3^{2-} and HPO_4^{2-} as well as the Na^+, Mg^{2+}, and K^{2+} in crystal lattice made its stoichiometric ratio is non-corresponding to the theoretical stoichiometric of the HA (1.67). Due to the different chemical composition of the mineral phase, the carbonate hydroxyapatite exhibits a poor crystallinity and provides the higher solubility compared to the stoichiometric HA. Around 90% of the natural bone organic phase is type I collagen. A small number of non-collagenous proteins (NCPs) and lipids are presents at around 5% and 2% by weight, respectively (Boskey, 2007; Young, 2003).

Bone can be divided into three main parts, periosteum, osseous tissue, and endosteum. For the first component, periosteum is the outermost bilayer membrane that responses for bone apposition during growth and development. Moreover, it is a key structure in blood supplying system for bone. It plays a major role on the bone remodeling process.

The second component is the osseous tissue with highly mineralized that attributes to the structural supporting function. According to the morphological characteristic, this component can classify into the dense part called cortical bone and loose part called cancellous bone. The cortical bone is composed of the solid matrix containing a series of voids (Haversian canals, Volkmann's canals, lacunae, and canaliculi). While the cancellous bone is characterized as the highly porous network with a porosity between 50% to 90% made from the connection of the small pieces of the trabeculae bone plates

9

(Rho et al., 1998). This mineralized matrix provides various types of growth factors that regulates the osteogenic activity (Hauschka et al., 1986).

The last part of bone structure is endosteum. It is a very thin layer of a connective tissue and cells. It is the part of periosteum which is engulfed by the newly formed osteon during the bone appositional process. The vessels in the engulfed periosteum become the Haversian blood vessels that nourish the osseous tissue, while the periosteum turns to the endosteum lining the Haversian canals and medullary cavities (Le et al., 2017). Because this structure houses the osteoprogenitor cells, then it contributes to bone regenerative mechanism. However, this tissue is less attractive for regenerative medicine because of its thin and indistinct appearance. The illustration of bones and its microstructures as well as cellular components of bone are showed in Figure 1.3.
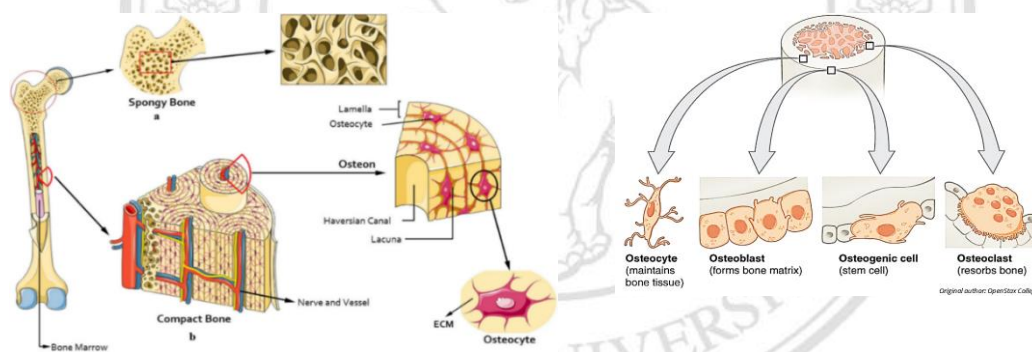
Figure 1.3. The illustration shows the components of bone, (i) cancellous and (ii) cortical bone (a). Note: the formation of haversian system which is made up of nerve, blood vessel, and osteocyte in the cortical bone (Amirazad et al., 2022). The various types of bone cells at each part of bone (b).

1.2.2 Alveolar bone and bone healing process

The bones related to oral cavity are maxilla and mandibles. They can be categorized as compact (cortical) and cancellous (spongy) parts according to the microarchitectures same as the bones in the other parts of the body. The maxillary and mandibular bones are

10

divided into three main parts (i) the body of mandible and maxilla (basal bone); (ii) the bone around the roots of the natural teeth (alveolar process); (iii) and the bone that lines inside the alveolar tooth socket and extends coronally to form the crest of the buccal bone (bundle bone). The components of the alveolar bone socket are presented in Figure 1.4.
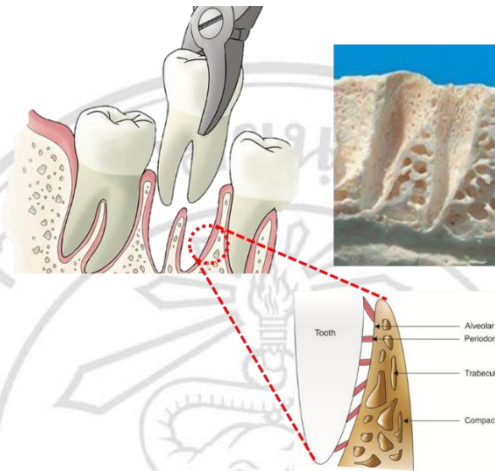
Figure 1.4. The morphology and structures of the maxilla and mandibular bone. The cortical and cancellous bone as well as the bundle bone with the insertion of periodontal fiber (Sharpey's fiber) from the periodontal ligament are exhibited.

The morphology and contour of alveolar bone is determined by the existing tooth at that area in the aspect of root size and shape, the position in dental arch, and tooth inclination. The previous study reported the average thickness of buccal bone plate at anterior tooth at only 0.5 mm that probably contributes to the significant alveolar bone contour alteration following tooth extraction in anterior part of maxilla (Januário et al., 2011).

When the natural tooth is removed, the remodeling of the extraction socket is initiated by the resorption of the bundle bone (Boyne, 1966) followed by the gradually resorption of the alveolar bone at an average of 0.5–1.0% per year throughout life (Ashman, 2000a; Devlin & Sloan, 2002). This remodeling process results in the reduction of alveolar bone height and the development of the concavity on buccal side of the ridge. The alveolar bone shrinkage in height and width around 40% to 60% is expected within the first 2-3 years after tooth removal (Ashman, 2000b).

11

The bone remodeling following natural tooth loss can be divided into two phases. First, the bundle bone located at the bottom of the extraction socket is rapidly resorbed leading to a significant reduction of the buccal aspect inside the socket. Then, the resorbed bone is replaced with the non-mineralized bone matrix consists of the irregular arrangement of collagen fibers and cells called woven bone (Araújo & Lindhe, 2005).

For the second phase, the remodeling of the outer surface of the alveolar bone is performed. This process causes the horizontal and vertical tissue reduction. The systematic and the physiologic factors such as the decreasing of blood supply in the extracted socket, the localized inflammation process, or trauma during the surgical procedures might play the important roles on accelerating of bone remodeling process following the natural tooth removal (Garetto et al., 1995).

Osteoblast, and the osteoclast are the cells that involve and play an essential action on the bone remodeling process. Various types of cells including the mesenchymal cells (MSCs), pre-osteoblasts, mature osteoblasts, bone-lining cells, and osteocytes are the osteoblast lineage which related to formation of new bone. On the other hand, the macrophages, osteoclasts, and multinucleated giant cells are classified as the osteoclast lineage which play a major role on bone resorption process (Corral et al., 1998).

The bone remodeling process is initiated when the mineral and bone matrix are destroyed by osteoclast cells. Then, the mononuclear cells will prepare the bone resorbed surface to enhance the osteoblast cell adhering, differentiating, and synthesizing the bone ECM for newly bone matrix formation in the next step. To complete the cycle, the newly formed bone matrix will be mineralized, and some osteoblasts will turn to osteocytes and embed in the new osseous structure. The balance between the formative and destructive process is critical for maintaining the healthy, structural integrity, and functionalize of skeletal system (Kular et al., 2012). The diagram of bone remodeling process is presented in Figure 1.5.
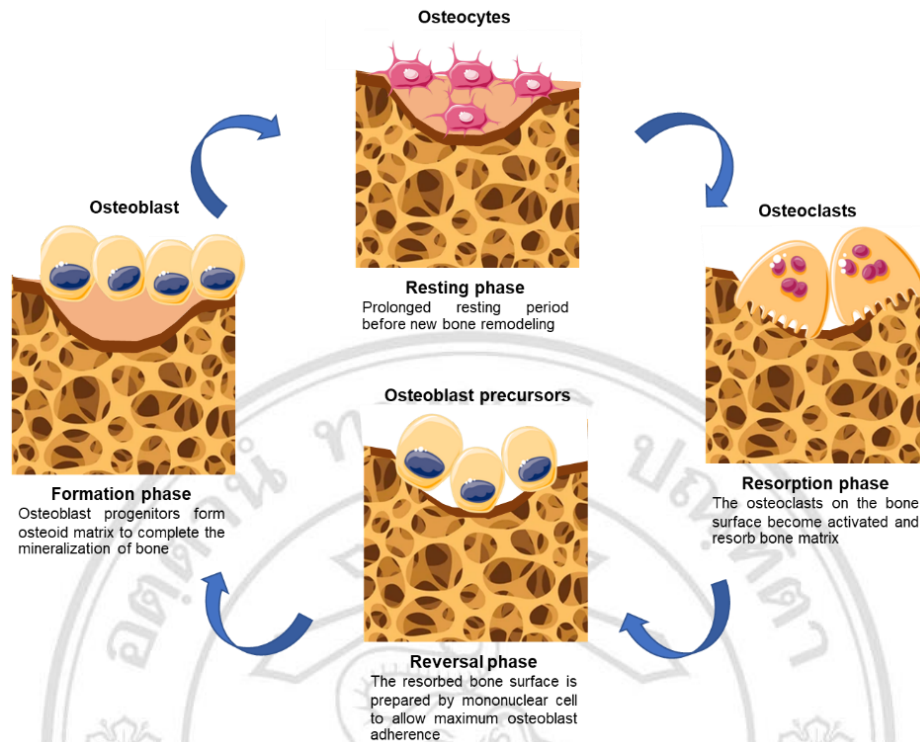
Figure 1.5. The schematic exhibits the bone remodeling cycle (Trombelli et al., 2008).

1.2.3 Tooth socket healing

After tooth removal, the series of the sequential histological changes of hard and soft tissues for socket healing have been initiated. This mechanism can be categorized into three phases including (i) inflammatory phase, (ii) proliferative phase and (iii) remodeling phase.

Inflammatory phase

This phase represents the response of body to the injury. It involves the formation of blood clot to stop the bleeding and the migration of inflammatory cell to initiate the inflammatory process. The contraction of vessels to reduce the blood supply at the extracted site and the sealing of leakage vessel with fibrin gel are performed to stop the bleeding. The necrotic blood clot inside the extraction socket is eliminated within next few days by the inflammatory cells. Then, the initiation of the new tissue formation is progress.

13

After the initial degradation of blood clot at the marginal portion, the mesenchymal cells from the remaining periodontal ligament (PDL) lining at bundle bone, the inflammatory cells, and vascular sprout cooperate to form the granulation tissues inside the tooth socket. Within one week after tooth extraction, the blood clot is almost completely replaced by the newly formed granulation tissue.

Proliferative phase

Following the formation of granulation tissue, the provisional matrix and the woven bone have been created. At first, mesenchymal cells from the residual principal fibers of the remaining PDL on bundle bone migrate and gather in granulation tissue to form the provisional matrix that composes of densely pack mesenchymal cell, collagen fiber and blood vessel with small or no inflammatory cells. Subsequently, the vessels and bone forming cells penetrate the provisional bone matrix and form the Woven bone which characterized as the fingerlike projections immature bone cell embedded in a primary spongy matrix. This step is almost finished within 6-8 weeks after tooth extraction.

Remodeling phase

The last phase of bone healing is the replacement of Woven bone with mature bone types. The minerals deposition into Woven bone results in formation of lamellar bone or bone marrow which classified as mature bone. At this step, the osteoclast cells been stimulated to regulate the equilibrium between bone formation and resorption to initiate the bone remodeling process. The bone maturation may take several months and exhibits substantial variability among individuals.

Although the bone modeling process inside the extracted socket is occupied evenly on the buccal and lingual walls as well as the outer and inner portions of the socket. But the greater shrinkage of alveolar bone contour is obviously observed vertically because the easy resorption of the thin buccal plate compared to the wider buccal bone. In addition, the earlier taking place of the bone modeling in bone healing process is also leaded to the significant reduction of alveolar bone contour at the first 3 months following the natural tooth loss (Schropp et al., 2003). At the end of the socket-healing process, the socket

14

entrance is filled with matured bone and covered by firm epithelial soft tissue. The illustration for tooth socket healing process is exhibited in Figure 1.6.
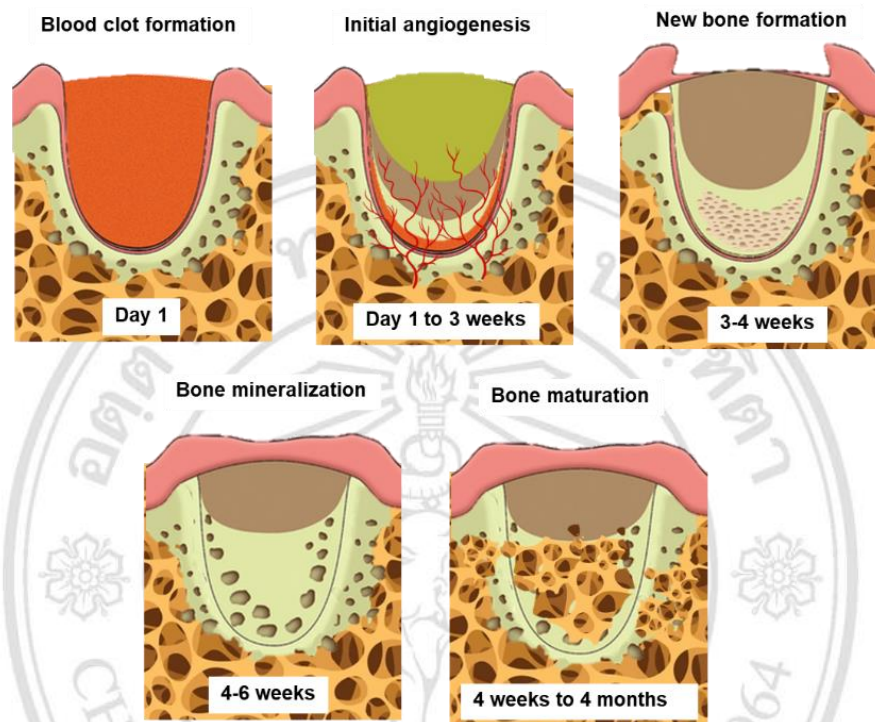
Figure 1.6. Schematic of the progression of the extraction socket healing process.

The expected time for completion of the tooth socket healing is a broad variation among individuals. Generally, the socket entrance may be closed within 10 to 20 weeks (Schropp et al., 2003). The expecting period for the presence of the radiographic finding in the extraction socket is between 3-6-months after tooth removal (Trombelli et al., 2008). According to the histological investigations, the formation of immature bone in the apical two-third of the socket is expected at 10 weeks and the complete of mature bone formation is observed at 15 weeks (Guglielmotti & Cabrini, 1985; Simpson, 1969).

Because of the esthetic interference due to the alveolar ridge volumetric contraction following natural tooth loss, grafting the tooth extracted sockets with different biomaterials have been proposed to limit this alteration. Although the immediate filling of tooth extraction socket with bone substitutes materials cannot inhibit the progression of bone remodeling process but this approach provides the enhancing effects on new bone

15

formation that resulted in the better preservation of the alveolar ridge dimension following tooth removal (Araújo et al., 2008; Araújo & Lindhe, 2005; Araújo & Lindhe, 2009).

1.2.4 Bone tissue engineering

The term "tissue engineering" was first used in 1987 (Langer & Vacanti, 1993). This concept bases on the combination of a three main factors, scaffold, living cells, and/or biological signals, to form a tissue engineering structure to enhance the tissue repair or regeneration (Hutmacher, 2000; Hutmacher et al., 2007). The attempt to restore the defective bone tissue by applying the synthetic bone graft material, calcium phosphates, to substitute the bone defective area was documented in the early nineteenth century (Dorozhkin, 2013). Since then, filling of the bone defect with the synthetic bioactive material as the temporary framework for cells to regenerate the bone morphology and functions called the bone-tissue engineering have been emerged as the new and promising strategy for bone restorative approach in modern medicine and dentistry.

Ideally, a bone scaffold should have the three-dimensional porous structures with high porosity and well interconnected pore network for cell growth and exchanging of nutrients and metabolic waste products. It should be the biocompatible and bioresorbable with a controllable degradation rate that corresponded to cell/tissue formative rate. Moreover, its surface morphology and surface chemistry should be suitable for cell to attach, proliferate, and differentiation. In addition, the scaffold should exhibit the compatible mechanical properties with the surrounding tissues at the recipient site (Huo et al., 2021). Nowadays, the advances in material science and the progression in cell biology as well as the material manufacturing process expand the boundary and break some limitations of the research in this field.

As mentioned in previous articles, the mimicking of the hierarchical structure of native bone, porous architecture, biological signals, and bone chemical composition are the significant aspects on the development of the biomaterial for bone-tissue engineering (Huo et al., 2021).

1.2.5 Bone biomaterials

The restoration of the osseous defects by the autogenous bone graft is currently accepted as the gold standard treatment option for both the medical and dental scenarios. In some situations, the xenograft or allograft has been recommended as the alternative to overcome the significant disadvantages of autograft including the surgical complications from the bone harvesting process, the donor-site morbidity, the limitation on bone quantity at the donor site as well as the negative effects on the patients' quality of life. However, the risk of disease transmission, immune rejection, and material cytotoxicity due to the material sterilization process still be the significant drawbacks of these alternative bone substitute materials (Kumar et al., 2013; Zhao et al., 2021). To achieve the successful in tissue regenerative approach and avoid the complications from the utilizing of conventional bone grafts , the applying of synthetic biomaterials which exhibits the same properties as the natural bone may be the promising solution (Polo-Corrales et al., 2014).

The recent advances in biotechnology have enabled the development of various types of materials for bone regenerative approaches. The ideal synthetic bone substitute materials should basically act as the supporting structure for cells, they could also provide the microenvironment and regulative signals toward bone cells to enhance the bone healing and regenerative mechanisms (Green et al., 2003).

From the literatures, the proper biomaterial for bone regenerative purpose should basically designed in 3D porous architectures with the specific properties to simulate the characteristics of natural bone structure. In addition, the bone scaffolds should have the osteoinductive and osteoconductive properties to accelerate bone regenerative mechanism by enhancing bone cell adhesion, proliferation, migration, and differentiation. In some scenarios, scaffold should be the carrier for biological signals, medicine, or engineered bio-substance for specific purpose (Chocholata et al., 2019; Ghassemi et al., 2018). These properties must be concerned in the development of the synthetic bone scaffold for bone regenerative purpose.

17

To optimize bone biomaterial, the character of natural bone in the aspect of composition, structure, and function should be mimic. The dissimilarity in microstructures may lead to the difference in cell responses, ECM formation, nutrient transport including the ingrowth of nerve and blood vessel into the synthetic scaffold (Fedorovich et al., 2011). The synthetic scaffold must have permeability to facilitate cell growth, migration, including the nutrients and oxygen exchange.

It is generally accepted that adequate porosity with appropriate pore sizes, as well as interconnectivity between each porous structure in the scaffold, are essential for bone regeneration. Scaffolds with inadequate porosity result in the restriction of cell migration and nutrient distribution, including waste product removal. On the other hand, a scaffold with a large pore structure leads to a reduction in the specific surface area, which plays a major role in cell adhesion, proliferation, and extracellular matrix formation (Baptista & Guedes, 2021).

The fabrication of three-dimensional porous architectures with different diameters ranged from nano to micro scale is another significant aspect that needs to be concerned in fabricating the ideal bone scaffold. The multi-scale porous structure not only increases the binding site for bone cells but it also enhances the cell bioactivities through the effect of microenvironment factor (Gao et al., 2017). The previous article addressed the positive effect on bone growth at the deep part of the synthetic scaffold with pore diameter of 150-800 µm (Wu et al., 2014).

Besides the significance of the scaffold physical morphology, the positive interaction between bone biomaterial and bone cells is the other major factor that plays a major role on the success of the bone regeneration. Basically, the synthetic bone scaffold should have the ability to guide the bone cells to grown on the scaffold that referred to the osteoconductive property as well as the ability to recruit the osteoprogenitor cells from remoted area for new bone formation which referred to the osteoinductive property (Albrektsson & Johansson, 2001; Kolk et al., 2012).

In summary, the optimal bone scaffold should not replicate only the porous bone microarchitectures, but it must also duplicate the chemical composition and biological

signals found in the native bone tissue. To achieve these requirements, various functionalization protocols that facilitated the material bioactivity such as the incorporating of osteoinductive growth factors or combining the calcium phosphate component are performed to overcome the inherent biological inert property of synthetic scaffold (Huo et al., 2021). However, these approaches cannot completely replicate the property of natural bone extracellular matrix.

1.2.6 Biopolymer for Bone scaffold

Because of the limitations on the conventional bone substitute materials, the application of the synthetic scaffold to regenerate the defective structure based on tissue engineering concept is considered as the promising approach for bone regeneration. Nowadays, the porous biomaterials with engineered properties are becoming a practical alternative option to the traditional bone repairing processes (Burdick et al., 2013). The word "biomaterials" was first mentioned in the early 1960s (Burny et al., 1995).

The history of biomaterials development for tissue scaffold can be categorized into three main generations. The first generation of biomaterial was started at the 1960s. At that time, the attention was mainly focused on achieving the compatibility of the biomaterial performance to the replaced structure as well as the formation of well material biocompatibility and less reactions to the host system. The first-generation biomaterials were generally bioinert and no biological interaction with surrounding tissue. It mainly focuses on the titanium, titanium alloys, polymethylmetacrylate (PMMA), poly (ether ether ketone) (PEEK), and ceramics such as alumina and zirconia.

Since the 1980s, the biomaterials had been used as the based material to fabricate the temporary framework for cells in tissue engineering called scaffold (Skalak & Fox, 1988). Because of the prerequisite requirements on biocompatibility and bioactivity of the cell scaffold, the development of bioactive property of the biomaterials as well as the *in vivo* biodegradable characteristic are considered as the crucial aspect in the second generation of biomaterial. At that time, the synthetic and natural polymers, calcium phosphate, calcium carbonate, calcium sulfate, and bioactive glasses were extensively investigated. Nowadays, we are in the era of the third-generation biomaterial. For this generation, the

19

improvement on specific biological properties of the second-generation biomaterials according to their specific applications to fabricate the biomaterial with outstanding performance is the main goal in biomaterial development. To achieve this requirement, the combination of the biological factors, external stimuli, or designing of specific surface microenvironment of the biomaterial are generally addressed (Yu et al., 2015).

According to the biomaterial generation which explained above, the modern bone biomaterial should have the same physiological architectures as the natural bone extracellular matrix to provide the suitable micro-environment for bone cells during the tissue regenerative process. In addition, it should provide the regenerative signals to regulate the related cells as occurred in the nature bone extracellular matrix during the bone healing process (Gao et al., 2017).

According to this reason, the various biomaterials including the synthetic and natural or the biodegradable and non-biodegradable materials have been applied as the matrix for porous bone scaffolds because they provide more controllability on both the physiochemical, biological characteristics and processability (A. Bharadwaz & A. C. Jayasuriya, 2020; Biswal, 2021). Basically, the proper scaffold-based biomaterials for bone tissue engineering must be compatible to the host cells and they must be the non-immune stimulating material (Lloyd, 2002). Furthermore, the materials degradation rate should be coincident with the healing period of the defective tissue, the mechanical properties should be corresponded to the specific applications, the material degradative by products should be non-toxic and can be easily eliminated from the body, the optimized material should have high surface hydrophilicity and high permeability to facilitate cell behaviors. In addition, the optimized materials should provide the versatility in material design and manufacturing (Saini et al., 2016).

According to the previously mentioned material requirements, the various type of metals, ceramics, and polymers have been investigated. Of these materials, the polymers possess an outstanding due to their facile and versatility in material processing and design. Moreover, their high biocompatible property and the biodegradative behaviors made them be promising material for applying in tissue engineering. For these reasons, the polymers especially the biodegradable type are the dominant scaffolding materials for tissue

20

regenerative purposes (Place et al., 2009). The possibility on the development of immunological reaction when applying the naturally derived polymer such as collagen, gelatin, or silk as the base material for tissue scaffold and their complicated structural composition have driven the interest of researchers for developing the synthetic polymers as the alternative choice for scaffolding materials (Lei et al., 2019; Place et al., 2009).

The synthetic aliphatic polyesters such as poly(lactic-acid)(PLA), poly(glycolic-acid)(PGA), poly(caprolactone)(PCL), including their copolymers are the most commonly utilized polymers for bone tissue engineering (Zhu et al., 2020). The presence of the ester functional group (R-CO-OR) in every repeat unit of the polymer main chain is the unique characteristic of materials in this group. These polymers can be classified into two major groups according to the molecular structure, aliphatic (linear) polyesters and aromatic (aromatic rings) polyesters. The category and materials in each group are presented in Figure 1.7.
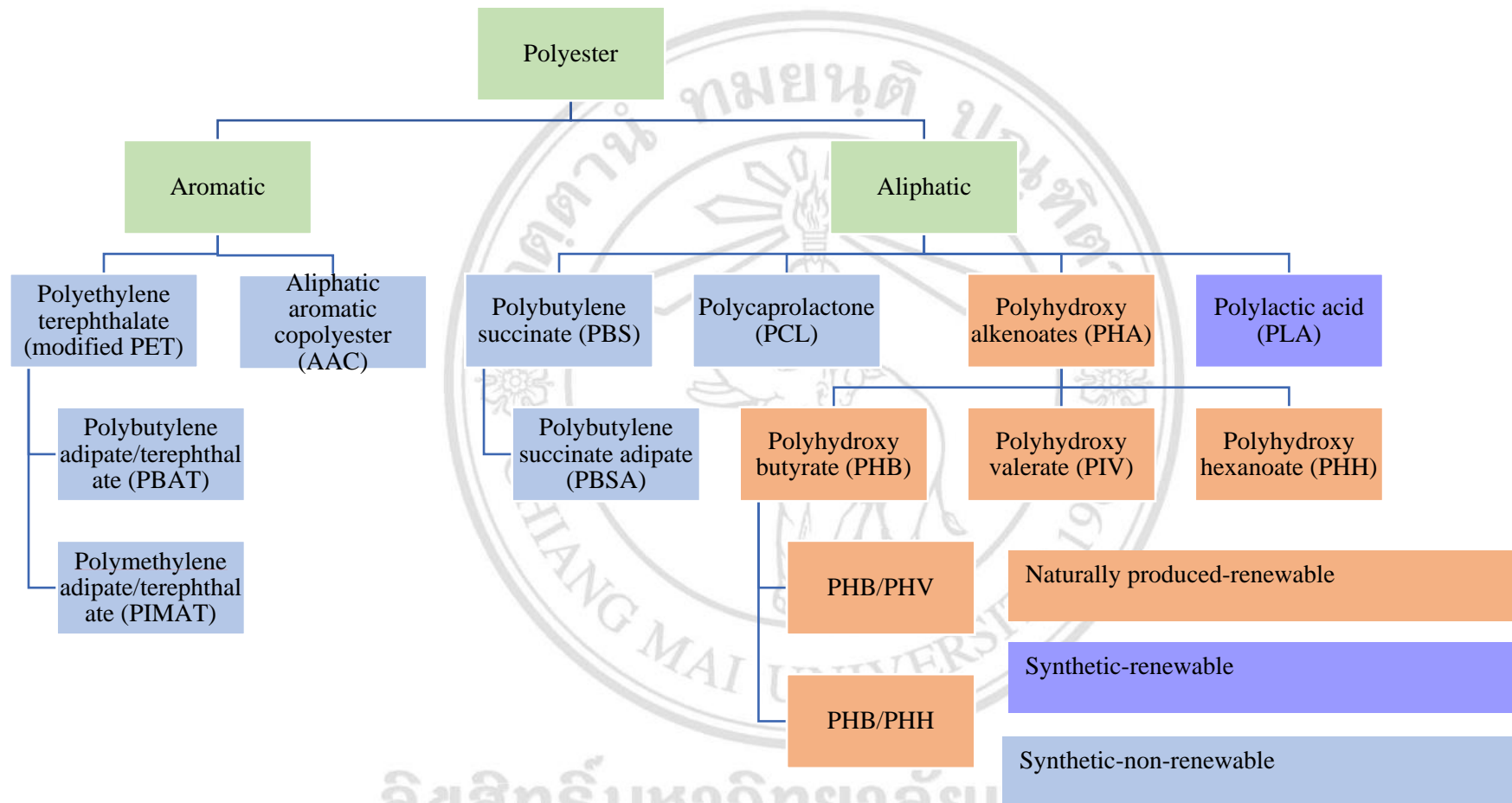
Figure 1.7. The diagram of polyester polymers (Nair & Laurencin, 2006, 2007; Nampoothiri et al., 2010)

The aliphatic polyesters are the most frequently used synthetic biopolymers for tissue regenerative purpose especially the one with biodegradative behavior. The aliphatic polyesters are basically defined as the long chain polymer with repeated units of the ester functional groups. The long chain polymer in the aliphatic polyester is a compound which all the carbon-carbon bonds are single bonds (Figure 1.8a). While the ester refers to the functional group which a carbon atom contains a double bond to an oxygen atom, and a single bond to a second oxygen atom (Figure 1.8b). The presence of the aliphatic ester bond in the polymer backbone leads to the bulk erosion that causes the gradual biodegradation in physical environment (Gopferich, 1997). The example of the commercially available biobased polyester that commonly applied in tissue engineering are polylactic acid (PLA), polyglycolic acid (PGA), poly-ε-caprolactone (PCL), polyhydroxybutyrate (PHB), and poly(3-hydroxy valerate).
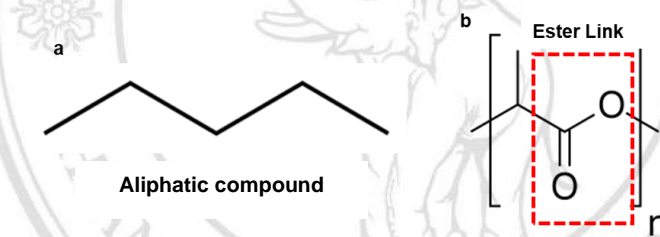
Figure 1.8. The diagram represents a simple structure of an aliphatic polyester . The simple structure of aliphatic compound (pentane) which made from all single carbon-carbon bonds (a). The ester functional group in the molecular structure of poly(lactic acid) (b).

1.2.7 Polylactide (PLA)

Lactic acid (LA) is a naturally occurring compound. It can be synthesized by the fermentation of corn, beets and carbohydrates from other crops (Inkinen et al., 2011). Approximately 90% of lactic acid production worldwide is made by bacterial fermentation while the remaining is synthesized by the hydrolysis of lactronitrile (Adsul et al., 2007). Due to its renewability, recyclability, biodegradability and composability, this biopolymer provides the promising capability to substitute the conventional

petroleum-based polymers in several industrial applications including the tissue engineering.

Many advantageous including the biodegradability, thermal plasticity and proper mechanical properties especially the excellence biocompatible toward many types of cells (Cheng et al., 2009) made PLA is one of the most widely used polyester for medical purpose (Pang et al., 2010). It has been applied for dissolvable surgical suture, bone fixing device, drug delivery device, and the material for tissue engineering. The degradation of PLA is dependent on the physiological conditions, especially pH and temperature, and polymer compositions (Xu et al., 2011). This property enables to tailor the material degradation rate to the desired clinical application.

The formation of non-toxic by products, lactic acid and carbon dioxide following the hydrolytic degradation in physiological environment is the second reason of making this polymer and its composite are good candidates for medical and pharmaceutical applications (Abd Alsaheb et al., 2015). The previous article stated that the degradative products of PLA caused by the hydrolysis of the ester-bond backbone are finally eliminated from the body as carbon dioxide gas and water (Da Silva et al., 2018). The investigation of the radiolabeled PLA degradation products confirmed the byproducts are secreted out of the body system, and not retained in the primary organs (Kulkarni et al., 1966). It assumes that the elimination of lactic acid and carbon dioxide occurs through the kidney filtration and urine.

The monomeric unit of PLA is lactic acid with the formula $CH_3–CH(OH)–COOH$. It has two enantiomers, $L(+)$- and $D (-)$-lactic acid, differing in their effect on polarized light. Depending on the different lactide steroismers, three different PLA materials can be expected such as poly(L-lactide) (PLLA), poly(Dlactide) (PDLA), or a racemic mixture called poly(D,L-lactide) or PDLLA. The sterioforms of the lactides are showed in Figure 1.9.

24
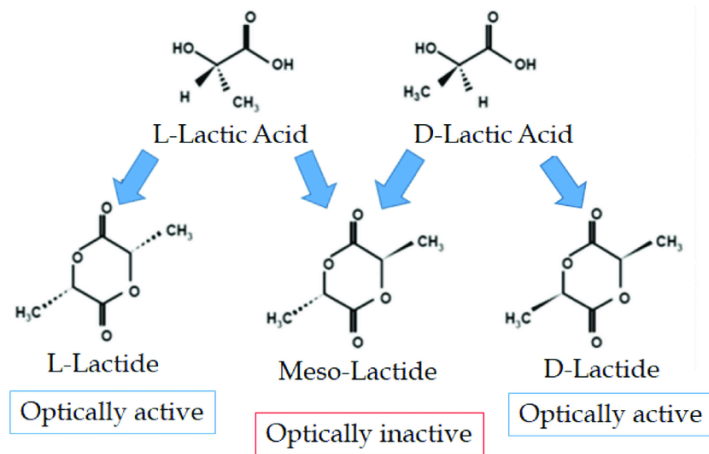
Figure 1.9. Steroforms of lactides (Teixeira et al., 2021).

Most of the commercially available PLA is the copolymers of PLLA and PDLLA (Lim et al., 2008; Teixeira et al., 2021). The stereoisomers of PLLA and PDLA are crystalline, whereas the PDLLA is amorphous. PLLA is a slow crystallizing, semi-crystalline polymer with crystallinity, melting, and glass transition temperature values ranging from 40% to 50%, 55–80 °C, and 170–180 °C, respectively (Lasprilla et al., 2012; Migliaresi et al., 1991). For PDLA, the polymer has crystallinity, melting, and glass transition temperature values ranging from 30% to 45%, 40–50 °C, and 120–150 °C, respectively (Sarasua et al., 2005). Both PLLA and PDLA have comparable tensile strength (4–8 GPa), elongation at break (1–8%), and tensile strength values (40–70 MPa) (Perego et al., 1996; Sarasua et al., 2005).

The data from *In vivo* studies revealed that the highly crystalline PLLA degrades completely in 2–5 years, whereas amorphous PDLLA loses its strength in less than 2 months and completely degrade within 12 months (Nair & Laurencin, 2007). Because of the long degradation times and the high crystallinity of the PLLA and PDLA can stimulate the inflammatory reaction then the utilizing of PDLLA polymer which has rapidly degradation and less crystallinity is more favorable for tissue engineering purposes (Fukushima & Kimura, 2008).

25

Although PLA is a good candidate for biomaterial in tissue engineering, but some inherent drawbacks such as the lower hydrophilic property and the material brittleness, are significant aspects that restricted the clinical applications. Therefore, the application of pure PLA polymer as the matrix for tissue engineering scaffold may not enough to achieve all requirements of the optimize the bone biomaterial.

To overcome this problem, the material modification by copolymer or composite development as well as surface functionalization could be concerned (Farah et al., 2016). Several approaches had been introduced to modify the characteristic and properties of PLA polymer including the copolymerization with other monomers, mixing with other compatible polymers or the incorporation with the appropriate biomaterials substance or particles (Mohapatra et al., 2014). In recent years, the application of PLA polymer composites has made a significant progression in bone tissue research. The various excellent properties of the biopolymeric composites, such as biodegradability and tunable mechanical properties(Liu et al., 2020; Tajbakhsh & Hajiali, 2017). Furthermore, the surface properties of the biomaterial are another aspect that provided a major effect on material application. Different surface modification techniques such as the physical, chemical, plasma, and radiation have been employed to engineer the desired surface properties of the PLA biomaterials.

Among the promising material modification approaches, the development of the composite that composed of bioactive-ceramic and biodegradable polymer provide a strong possibility to utilize as materials for bone scaffold in medical purposes (Latimer et al., 2021). This composite exhibits many advantages including the excellent in biocompatibility, biodegradative behaviors, bioactive property, and the osteogenic property. These advantages including their high versatility and facile in manufacturing and design as well as the simplicity in tailoring material properties to meet the specific requirements made the polymeric composite materials are attractive for tissue engineering (Baranwal et al., 2022).

26

1.2.8 Polybutylene adipate-co-terephthalate (PBAT)

The aliphatic polyesters are attracted by industries as the promising composable materials for various applications. However, the high production cost and the inherent unfavorable physical and mechanical properties are the significant limitations of this material. To overcome this drawback, the development of polymer that consists of both the aliphatic and aromatic units in the same polyester chain which exhibits the biodegradative property as the aliphatic polymers and provides the excellence physical and mechanical properties as the aromatic polyesters should be classified as the outstanding biodegradable polymer.

The aliphatic-aromatic co-polyesters consist in mixture of aliphatic and aromatic monomers can be produced by polycondensation reaction of 1,4-butanediol, adipic and terephthalic acids (or butylene adipate) (Okada, 2002). The complete biodegradative behavior, the excellence material ductility, and the very high elongation at break value at close to 700% comparing to the other biodegradable polyesters are the outstanding properties of the PBAT (Zarrinbakhsh et al., 2013). Therefore, the combination of this co-polyesters with other aliphatic polymers such as PLA, glycolic acid, and succinic acid is documented as the simple and effective technique to fabricate the new material with higher flexibility and toughness (Kondratowicz & Ukielski, 2009; Olewnik & Czerwiński, 2009; Soni et al., 2009).

Nowadays, the application of pure PBAT as the biomaterial for tissue engineering had been reported (Arslan et al., 2018; Liu et al., 2021). But, the poor thermal and mechanical resistance of PBAT are the major limitations toward the industrial and medical applications as bone implant (Fukushima et al., 2012). For this reason, it usually applies as the complementary polymer of PLA to improve the material ductility and toughness (Khatsee et al., 2018; Nofar et al., 2017).

1.2.9 PLA/PBAT blends for tissue engineering

The physical blending or mixing of at least two different polymers to create a new material with different physical properties had been interested as a simple and cost-effective approach for modifying the already existing polymers (Yu et al., 2006). The

27

rapid mixing protocol, less energy required, and the less exposure to the unfavorable chemical reaction are the major advantages of the material preparation by the polymer solution blend method (Nyamweya, 2021; Paul & Barlow, 1980). The properties of the resulted blends are determined by type of combining polymer and the polymer component ratio in the blend (Tipduangta et al., 2021).

Generally, polymer blends are classified into either miscible (homogeneous) or immiscible (heterogeneous) blends. The miscible polymer blend refers to a blend of two or more polymers homogeneous down to the molecular level and fulfilling the thermodynamic conditions for a miscible multicomponent system. On the other hand, an immiscible polymer blend means to the material that does not comply with the thermodynamic conditions of phase stability (Moustafa et al., 2017; S. Su et al., 2020; Tran et al., 2018).

For the immiscible polymer blend, the compatibility between the polymer phases significantly influences on the properties of a resulted polymer. The degree of the interactions between each phase in a polymer system play a major role on material properties and characteristics. The immiscible polymers blend which has the sufficiently strong interactions between each polymer component results in the formation of the macroscopically homogeneous character. Comparing to the polymer blend system with large interfacial tension on each polymer component, the formation of phase separation in the polymer blends system that causes the decreasing of mechanical properties is observed (Toh et al., 2021).

As the demands on new biopolymeric materials and their composites for tissue engineering has continuously increased over the years. The development on man-made polymeric blends that confer unique structural and mechanical properties as well as the biological characteristics for the specific application in medical and tissue regenerative purpose is the major challenging aspect for the researchers. To fulfill this objective, the intensive studies on developing new generation of biomaterial by the combination of biopolymer blends and bioactive substance are interested (Angshuman Bharadwaz & Ambalangodage C Jayasuriya, 2020).

28

In the last few decades, there has been a continuous growing of the interesting in the application of biodegradable plastic instead of the conventional petroleum-based polymer in various fields (Garavand et al., 2017). Among all biodegradable polymers, the PLA shows the promising possibility for applying as the biopolymer for tissue engineering due to its biocompatibility, biodegradable, and the approval from FDA (Food and Drug Administration) as safe material for contact with food (Ashothaman et al., 2021; Taib et al., 2022). However, the material's brittleness, the lack of cell recognition sites, and the absence of osteoconductivity are significant drawbacks that restrict the material's application in tissue regeneration (Nofar et al., 2019).

According to a previous article, the incorporation of a high-toughness compatible biopolymer such as polybutylene adipate-co-terephthalate (PBAT) into the PLA matrix can effectively improve the material's toughness and flexibility (Shen Su et al., 2020). This high-toughness PLA/PBAT blends has been commonly used for packaging or agricultural purposes (Pietrosanto et al., 2020; Zhang et al., 2019). Only a few studies have mentioned it as a biomaterial for tissue regenerative applications. Recent studies addressed the *in vitro* biocompatibility of a PLA/PBAT blend toward fibroblast cells. However, they concluded that the lack of bioactive properties was a significant drawback for its application clinically (Kang et al., 2018; D. Yan et al., 2020). To overcome this limitation, surface coating with bioactive substances in the inert polymer matrix has been considered as one of the simplest processes to improve the material's bioactivity.

1.2.10 PDA-assisted biomineralization Surface modification

Nowadays, the biodegradable polymer is widely accepted as one of the promising materials for implanted devices and tissue scaffolds. The material in this group shows many significant advantages such as the low synthetic cost, the simplicity in material properties modification, and the versatility in material design and manufacturing (Iqbal et al., 2019). However, some surface properties such as the deficiency of the free surface functional groups, the poor surface wettability, and lack of the specific topographical features that provide the positive effects toward the living cells are the major aspects that limit their ability in cells bioactivities enhancement including the bio-integration with the surrounding structures (Amani et al., 2019; Ferrari et al., 2019).

29

The surface engineering by creating the functionalized layer of the controlled chemical composition, microarchitectures, surface roughness, and surface wettability have considered as a simple and effective approach to overcome the inherent biodegradable polymer disadvantages. Moreover, the material biological improvement by surface engineering technique can be achieved without the significant alteration of the bulk properties of the implanted materials (Nothling et al., 2022; Wieszczycka et al., 2021).

Various forms of calcium phosphate (CaP) have been widely used as the bioactive substance for surface engineering of the bioinert polymers to mimic the physicochemical characteristics and microarchitectures that favored bone cells bioactivities and osteogenesis (Surmenev et al., 2014; Xiao et al., 2020). The biocompatibility as well as the osteoconductive and osteoinductive properties of CaP made this biomaterial is widely employed in bone regeneration for decades (LeGeros, 2008; Tang et al., 2018).

To deposit the CaP on the surface of bioinert polymer, many techniques have been introduced including the biomimetic mineralization (Shin et al., 2017). The biomimetic CaP coating process that mimics nature's biomineralization mechanism typically occurs at physiological temperature (~37°C) and neutral pH range overcomes many shortcomings of the conventional coating techniques which required the high processing and/or annealing temperature (Kokubo & Takadama, 2006).

The *in vitro* formation of CaP biomineralized layer on material surface by incubating a substrate in a supersaturated solution known as simulated body fluid (SBF) had reported by Kokubo et al. in 1990 (Kokubo et al., 1990). The high concentration of calcium and phosphate in these fluids promotes the formation of calcium phosphate (CaP) crystalline structures which has the chemical composition same as the apatite found in native bone. Such an approach can be performed on any surface characteristic including the specimens with irregularity and complicated porous architectures (Maia-Pinto et al., 2020; Xie et al., 2016). This technique is successfully deposited the bone-like apatite layer on various types of substrates including metals, ceramics, and biodegradable polymers. To accelerate the biomineralization process, the SBF solution at various concentrations (1.5 times (Tanahashi et al., 1994), 5 times (Wei et al., 2019) , and 10 times (Cai et al., 2011) compared to blood plasma) are applied. The studies suggested that the 10 times

concentrated SBF accelerated the formation of mineralized layers by providing a higher number of required ions. The modified 10X-SBF solutions can induce the homogeneous deposition of CaP mineral in as little as two hours (Chen et al., 2009; Tas & Bhaduri, 2004; Wan & Chen, 2011).

Because the SBF solution can easily penetrate to all areas of substrate, then this technique can form the CaP mineralized layer on the entire surface of substrate with a highly complex structure such as the three-dimensional interconnected porous scaffold. Furthermore, the coating process is performed under the biological friendly conditions in the aspect of temperature, pressure, and pH. Therefore, this technique can be performed on fragile and low thermal resistance substrates which are easily destroyed by conventional surface coating technique. In addition, the mild coating conditions also enable the potential combination of biomolecules such as proteins, growth factors and genes to the generated CaP mineralized layer (Riau et al., 2020; Shin et al., 2017).

The mechanism of CaP mineralized formation presented in Figure 1.10. First, the high concentration of calcium (Ca) and phosphorous (P) ions in SBF solution begin to form a prenucleation crystals. The amorphous particles in SPB solution are attracted by the polar surface functional groups of the substrate to form the apatite crystals. The deposited apatite is function as a nucleation site allowing for continue crystal growing (Tanahashi & Matsuda, 1997).
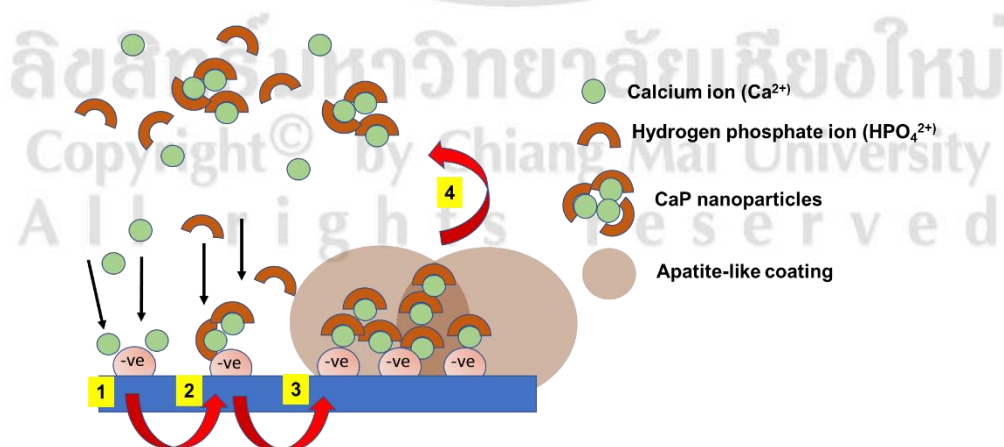
Figure 1.10. The SBF-mediated mineralization on material with negative charged surface. The calcium ions (Ca^{2+}) interact with the negative charged on substrate surface

31

and start the mineralization process (1). The accumulated Ca^{2+} ions attract the hydrogen phosphate ions (HPO_4^{2-}) to form the CaP nanoparticles (2). The CaP nanoparticles serve as a secondary nucleation site for continue apatite growth on the surface of substrate (3). The surface nucleation sites may attract the formation of CaP crystals in SBF (4).

However, the limited surface interaction between the biomimetic CaP layer made by biomineralization method and the polymer surface may be considered the major drawback of this technique. The previous article mentioned about the weaker interaction ability of the ordinary biomimetic deposition method to the titanium substrate (Weng et al., 1997).

To overcome this inherent limitation, the utilization of PDA coating layer as a bioactive and multifunctional anchoring platform for the nucleation, growth, and orderly formation of inorganic crystals on the surface of bioinert material called polydopamine-assisted biomineralization has been recommended (Ryu et al., 2010). The abundant catechol and amino functional groups found in the deposited polydopamine layer can provide the nucleation sites for hydroxyapatite and accelerate subsequent hydroxyapatite deposition (Ghorbani, Zamanian, Behnamghader, & Daliri-Joupari, 2019; Ghorbani, Zamanian, Behnamghader, & Joupari, 2019). Based on this behavior, Ryu et al. (Ryu et al., 2010) presented the simple procedure to immobilize the CaP apatite on various type of materials by the assistance of polydopamine (PDA) primer layer. They mentioned about the dual role of PDA layer, the molecular anchor for a wide range of surface substrates and the active binding site for Ca^{2+} ion.

Surface functionalization by polydopamine coating is a single-step and material-independent surface functionalization method that was first reported in 2007 by Lee and colleague (H. Lee et al., 2007). The versatility and the simplicity in manipulation made this approach is powerful for surface functionalization in various fields from the energy industrial to the biomedical engineering (Ho & Ding, 2014). The coating is inspired by the adhesive proteins secreted by sea mussels for adhering to the various inorganic and organic surfaces in the ocean. The high catechol (3,4-dihydroxybenzene) content and the high primary and secondary amine content as well as the histidine residues in the mytilus foot proteins-3 and −5 (Mfp-3 and −5) located in the distal portion of the mussel byssus play a major role on the solidification of mussel adhesive protein and the formation of the

32

strong covalent and noncovalent bond with substrates (Shin et al., 2022). The illustration of the mussel byssal plaque and its containing proteins are presented in Figure 1.11.
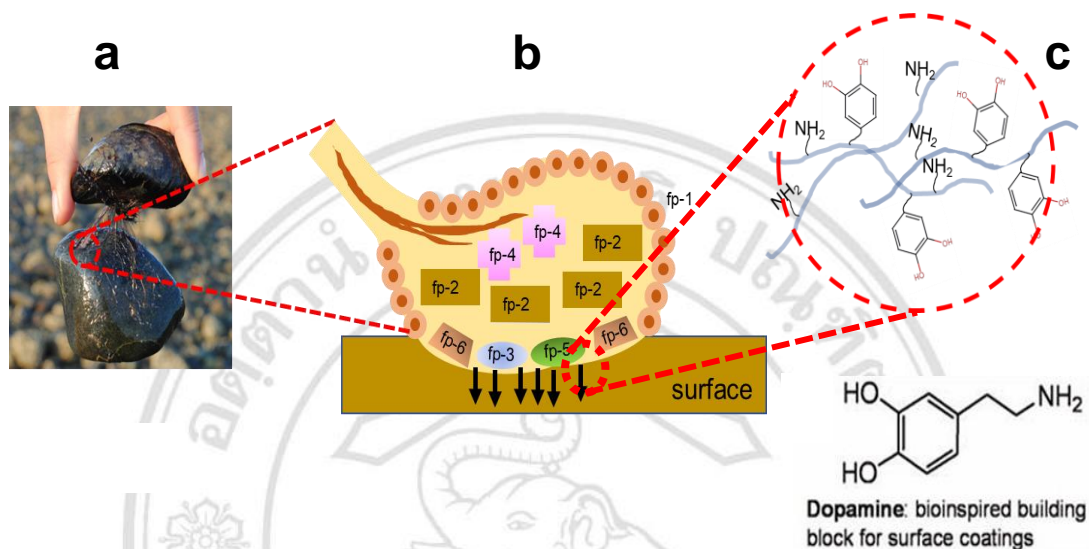
Figure 1.11. Schematic view of a mussel byssal plaque. The adhesive plaque is made at the distal depression on the mussel's foot (a). The molecular model of each plaque. Dopa-containing proteins nearest the interface are mfp-3 (fast and slow), mfp-5, and mfp-6 (b) (Nicklisch & Waite, 2012). The catechol and amine groups at the interface of mussel byssal plaque (c).

The mussel-inspired polydopamine (PDA) has been recommended as an organic platform to immobilize bioactive molecules or ions onto various types of surfaces (Wei et al., 2015). This thin film is generated through base-triggered oxidation and dopamine self-polymerization during the material's soaking in dopamine solution (H. Lee et al., 2007). Figure 1.12 exhibits the mechanism of PDA formation from the aqueous dopamine solution. It is commonly accepted that the intermediate indoles, 5,6-hydroxyindole and 5,6-indolequinone, play a significant role in the formation of the dopamine-based polydopamine. The resulted PDA is comprises of the oligomers of covalently bonded dimers and higher oligomers of 5,6-hydroxyindole and 5,6-indolequinone held by charge transfer and hydrogen bonding (Zangmeister et al., 2013). The strong and reliable PDA priming layer also improves the surface adhesion between the biomineralized layer and

the surface substrate that results in the durable bioactive coating layer (Murari et al., 2020).
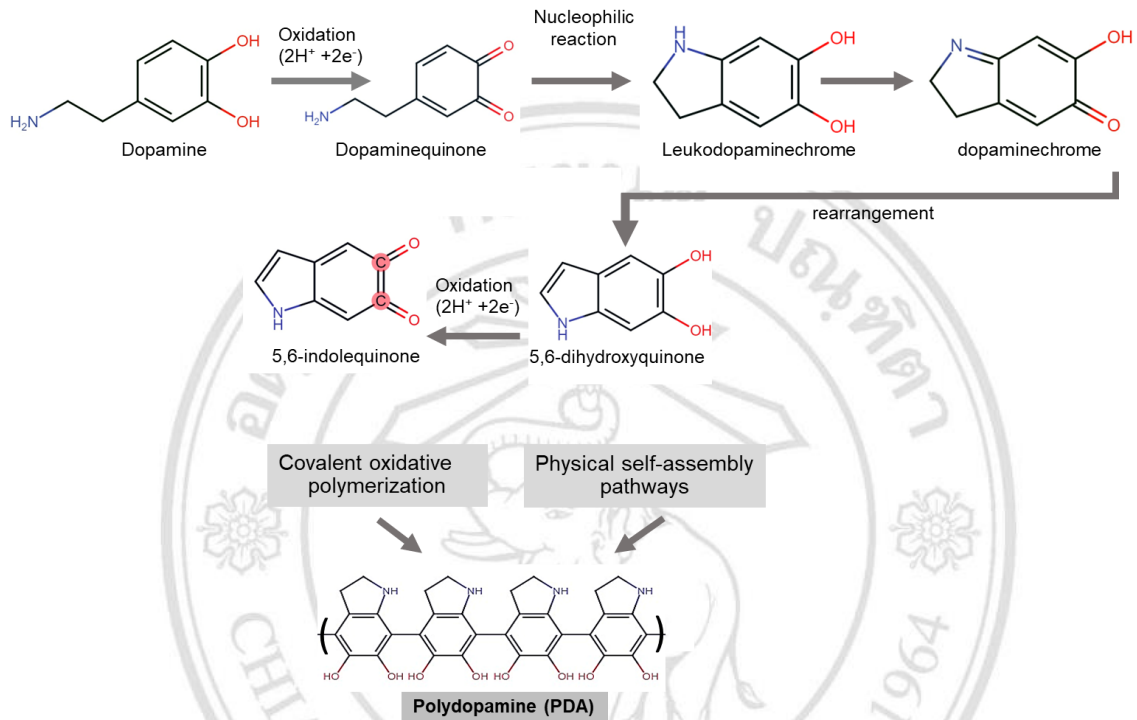
Figure 1.12. A schematic illustration of the reaction mechanism of polydopamine formation from dopamine (Jia et al., 2019; Haeshin Lee et al., 2007; Zangmeister et al., 2013)

The formation of the CaP biomineralized layer on the PDA-modified surface is initiated by the deposition of calcium (Ca^{2+}) ions on the PDA-coated surface through the accelerating effect of the surface negative charge induced by the catechol and amine functional groups on the PDA layer. The ionic interaction initiates the formation of the CaP biomineralized particle on the PDA functionalized surface. The progression of the layer-by-layer deposition of Ca^{2+} and PO_4^{3-} ions results in the formation of the CaP biomineralized layer, covering the surface of the substrate (Cui et al., 2016; Ghorbani, Zamanian, Behnamghader, & Daliri-Joupari, 2019; Palmer et al., 2008). A schematic of the biomineralization process is provided in Figure 1.13.

34
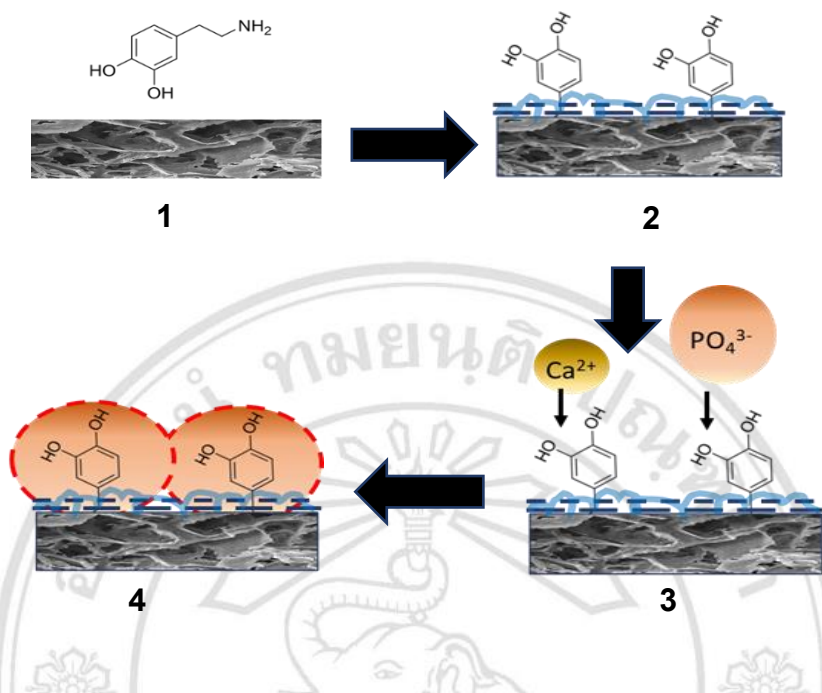
Figure 1.13. A schematic illustrating the procedure of biomineral deposition on a PDA-coated surface. (1) The self-polymerization of dopamine solution results in the formation of polydopamine (PDA) layer on the surface of the substrate. (2) The presence of the surface negative charge induced by the catechol and amine functional groups on PDA layer leaded to the accumulation of Ca^{2+} from the SBF solution. (3) The ionic interaction between the calcium ion (Ca^{2+}) and phosphate (PO_4^{3-}) results in the formation of the Calcium-phosphate biomineral. (4) the progression of the layer-by-layer deposition process results in the formation of bio-composites PDA-CaP mineralized layer.

The surface functionalization by the polydopamine-calcium phosphate apatite deposition is rapid and easy approach. The chemical properties as well as the useful features associated with bone tissue regeneration due to the presence of PDA layer are confirmed by both the previous *in vitro* and *in vivo* studies (Deng et al., 2019; Du et al., 2022). Its surface functional groups influence on the attachment of biomolecules including the interfacial properties that provide considerable effects on cell behaviors and new bone formation (Lynge et al., 2011). It has been discovered that the improvement on surface hydrophilicity due to the presence of PDA could encourage cell spreading and attachment on the scaffold surface (Liu et al., 2018; J. Yan et al., 2020).

35

When the bio-adhesive function of PDA layer has been applied as the platform for biomimetic surface mineralization or the biomolecule immobilization, the synergistic effect on new bone formation would be expected. The PDA-assisted biomineralization surface modification has gained much attention from the researchers as the method for improving both the physical properties and biological activities of the substrates (Kaushik et al., 2020). The formation of the relatively rough and irregular surface in nanoscale of the bioactive hybrid layer composes of the hydroxyapatite crystals, amorphous CaP apatite, and PDA results in the microenvironment that suitable for cells and bone regenerative process (Ohtsuki et al., 2007). The positive effect of the formation of surface roughness at the micro and subo-micro levels on osteoblast differentiation was mentioned in the earlier article (Gittens et al., 2011).

The previous study revealed that the deposition of the HA particles on the PDA platform resulted in the osteogenic differentiative enhancement *in vitro* and *in vivo* tests (Ko et al., 2017). The formation of PDA and HA on the outer surface of bio-inert materials, poly(caprolactone) (PCL), results in the obvious enhancement on the pre-osteoblast cells (MC3T3-E1) adhesion and proliferation. Moreover, this surface modification strategy also influences on the up-regulated alkaline phosphatase (ALP) activity as well as the osteogenic-related genes and proteins expression toward the MC3T3-E1 cells (Chen et al., 2019). The advantage on bone regenerating possibility made this technique is attracted for clinical applications especially for bone tissue engineering (Kaushik et al., 2020; Patra & Seeger, 2017).

The *in vitro* study shows the synergistic effect on metabolic activity, alkaline phosphatase activity, and calcium deposition when the PDA-assisted biomineralization surface modification is incorporated with bone morphogenetic protein-2 (BMP-2) (Park et al., 2021). The successful deposition of silk fibroin and its derived peptide on chemically oxidized titanium coated with PDA has mentioned in the previous article (Xu et al., 2021). These data indicate the multifunctional efficiency of the PDA layer in immobilizing the various types of bioactive molecules on the surface of bio-inert materials. Furthermore, the biological benefits from the combination of boosted surface hydrophilicity due to the presence of PDA molecules and the increasing of surface micro roughness following the biomineralization process (Kaushik et al., 2020) including the applicability in specimens

36

with high porosity or complicated morphological structures (Wang et al., 2021) are the other significant advantages that made this technique attractive for applying in bone regenerative purpose. The biological improvements cause from the introduction of PDA-assisted biomineralization are summarized in Figure 1.14.
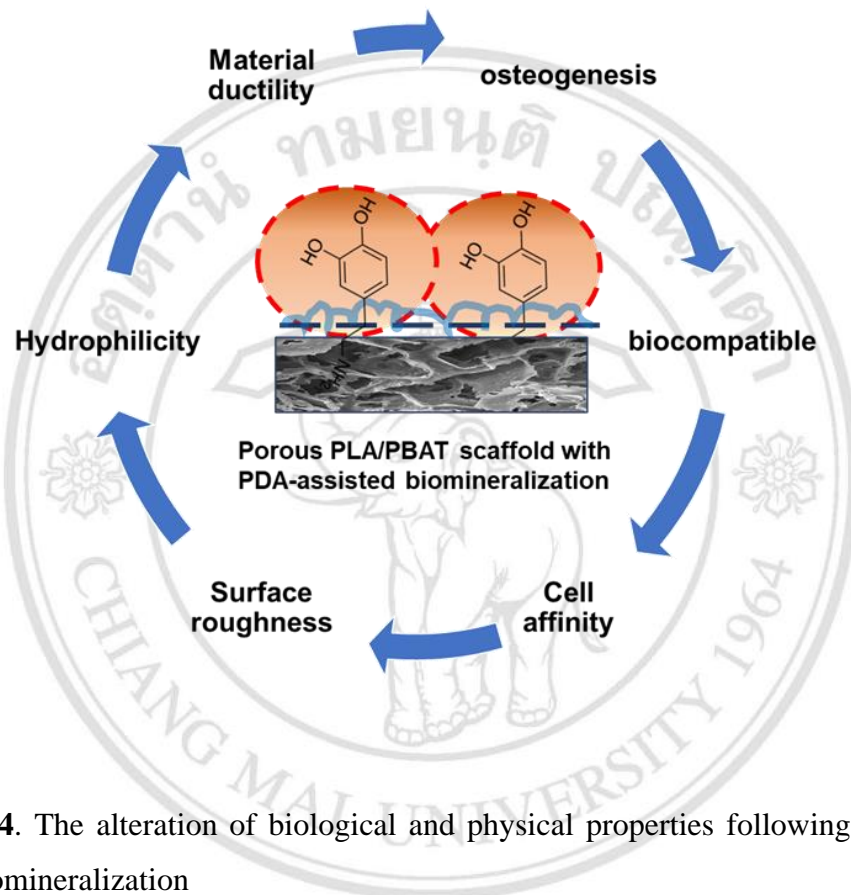
Figure 1.14. The alteration of biological and physical properties following the PDA-assisted biomineralization

CHAPTER 2

Research Articles

2.1 Published paper

2.1.1 Wattanuchariya, W. and Suttiat, K. (2022). Characterization of Polylactic/Polyethylene glycol/Bone Decellularized Extracellular Matrix Biodegradable Composite for Tissue Regeneration. Chiang Mai University Journal of Natural Science. 21(1): e2022008.

This study evaluates the potential possibility for applying the PLA composite, PLA with plasticizing agent (PEG) and porcine bone decellularization particles (bone dECM), as the biopolymer for bone tissue regeneration. The PLA/PEG/Bone dECM composite with various ratio of procine bone decellularized particles were successfully prepared by film casting technique. The increasing of surface irregularity and defects as well as the agglomeration of the dECM particles were observed when incorporating the bone dECM particles into polymer matrix. The incorporation of PEG into PLA matrix was significantly increased the degradation rate of PLA/PEG/Bone dECM composite especially when the bone decellularized particles reach to 10 wt% or 20 wt%.

The improvement on material hydrophilicity, biocompatibility toward the L929 cells and the *in vitro* osteogenic potential toward the human osteoblast like cell (MG-63) were observed on the specimens combined with bone dECM. The composite exhibits the potential possibility for applying as biodegradable material for bone regenerative purposes.

However, the rigidity of the polymer matrix and the agglomeration of bone dECM particles in polymer matrix as well as the separation of bone dECM particles when applying this composite for fabricating the specimen with porous architecture by gas

foaming/ammonium bicarbonate leaching technique are the significant drawbacks that limit the application in porous scaffold fabrication.

For this reason, the material modification strategy by depositing the outer surface of the scaffold with bioactive agent instead of the direct incorporation of bioactive agent into the polymer matrix has been investigated in the second study. We hypothesize that the surface modification technique could be the good candidate for improving the bioactivity and osteogenicity of the bioinert material because it could improve the material bioactivity without interfering the inherent properties of bulk materi
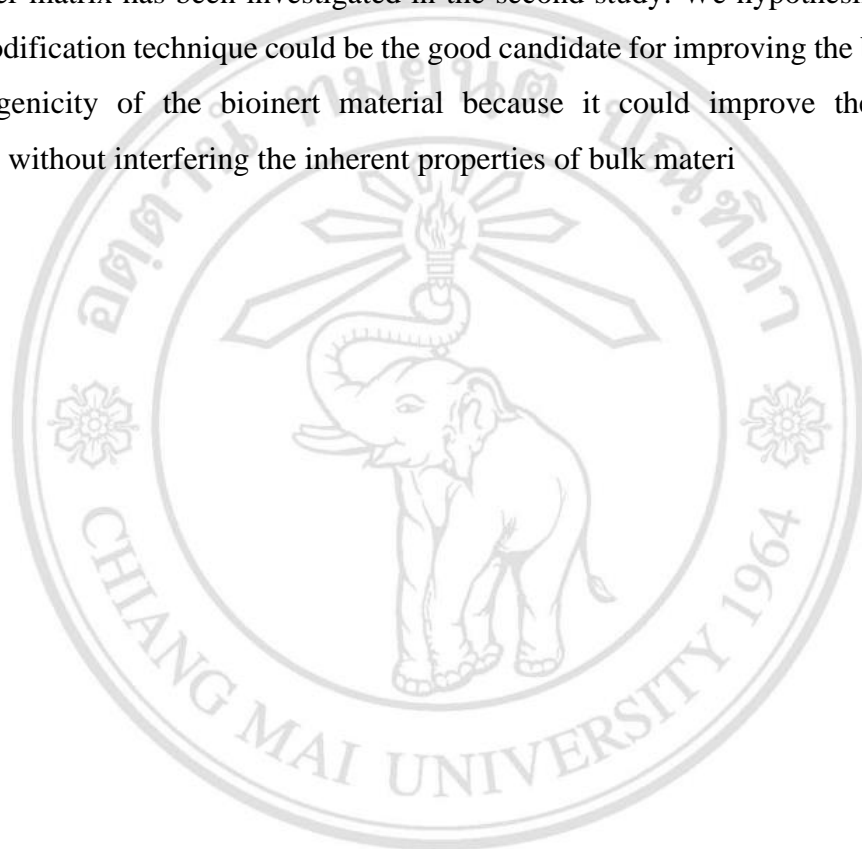
2.1.2 Suttiat, K.; Wattanutchariya, W.; and Manaspon, C. (2022) Preparation and Characterization of Porous Poly(Lactic Acid)/Poly(Butylene Adipate-Co-Terepthalate) (PLA/PBAT) Scaffold with Polydopamine-Assisted Biomineralization for Bone Regeneration. Materials, 15.7756 DOI: 10.3390/ma15217756.

In clinical scenario, the tooth socket filling materials with compressible property should provide the advantage over the rigid and brittle scaffold. The sponge-like biomaterial with little flexibility is more suitable for clinical applying in recipient sites with irregularly shape like tooth extraction socket. The tug back between the tooth socket filling material and tooth extraction socket leads to the increasing of the primary stability of the scaffold in the grafting site and maintain the tooth filling material in the recipient site. If the mechanical stability of the graft material does not adequate during the initial stage of bone healing process, the formation of the granulation tissue and fibrosis at the interface between graft material and implanted site could be observed (Bauer & Muschler, 2000). Therefore, the primary stability of the grafted material which related to the integrity of the new bone formation could be concerned in bone scaffold development.

Although our developed PLA/PEG/bone dECM composite exhibits the biodegradable property and the biocompatibility as well as the osteogenic potential toward the human osteoblast like cell, but the mechanical properties especially the material rigidity and brittleness including the agglomeration of bone dECM particles in polymer matrix are the major inherent drawbacks which limited the utilizing as the matrix for tooth socket filling material with opened porous structures. To overcome this problem, the application of flexible materials with biocompatibility as the matrix of tooth socket filling material for socket preservation is necessary.

In the second publication, the PLA/PBAT blend which exhibits the improvement on material flexibility and toughness is applied as the matrix for porous scaffold. To fulfil basic biological requirements of bone scaffold, the material bioactive property and the osteogenic potential are improved by the PDA-assisted biomineralization via the two-step simple dipping in dopamine solution with alkaline pH followed by the 10x-like SBF

solution. The characterizations of this such scaffold are presented in the second publication.

Besides the difference in resin matrix of the scaffold, the approach for modifying the biological properties of the porous scaffold is also modified. The depositing of bioactive composite layer on the outer surface of the scaffold instead of the direct incorporation of bioactive agent into the polymer matrix has been selected. We hypothesize that the surface modification technique could be the good candidate for improving the bioactivity and osteogenicity of the bioinert material because it could improve the material bioactivity without interfering the inherent properties of bulk material.

This study in the second publication aims to develop the synthetic polymeric scaffold which simultaneously provides highly porous architectures with well interconnected network and the osteogenic potential for applying as the alternative tooth socket filling material in socket preservation technique.

This study successfully prepared the highly porous scaffold with well interconnected porous architectures from the blend of biodegradable polymers, PLA and PBAT, by the application of gas foaming/ammonium bicarbonate particulate leaching technique. The improvement on bioactive and osteogenic properties of the prepared scaffold are simply performed by PDA-assisted biomineralization, the two steps dipping in dopamine (DA) solution with Tris-HCl at alkaline pH at room temperature followed by the soaking in $10\times$-SBF like solution to deposit the biomineralized CaP apatite on the entire scaffold surface.

The presence of the catechol and amine functional groups in PDA layer facilitates the deposition of Ca^{2+} and PO_4^{3-} ions from the $10\times$-SBF like solution to generate the CaP biomineralized layer on the PDA primed surface. In the present study, the formation of the bio-composite layer consisted of polydopamine (PDA), amorphous CaP and hydroxyapatite (HA) crystals significantly improves the scaffold surface hydrophilicity and bioactivity as well as the osteogenic property toward the human osteoblast like cell

41

(MG-63). The surface morphological alteration in nano level and the presence of PDA's functional groups as well as the formation of CaP biomineralization are hypothesized as the factors which play a major role on the osteogenesis potential in PLA/PBAT scaffold with PDA-assisted biomineralization.

The developing PLA/PBAT scaffold with PDA-assisted biomineralization also shows the improvement on the compressible property. The deformation of the scaffold without the fracture or breakage is observed under the compressive load. This character is beneficial for clinical application in recipient sites with irregular shape such as the tooth extraction socket. Moreover, the tugging between the bone substitute material and the defective bone lesion also plays a significant role on the primary stability of the porous scaffold in the recipient site.

According to the results from the present study, the developing PLA/PBAT scaffold with PDA-assisted biomineralization surface modification simultaneously presents the porous structures with well interconnected networks and osteogenic property to human osteoblast like cell are successfully prepared by the simple, cheap, and mild fabricating conditions called PDA-assisted biomineralization. The proper microenvironments for bone cells such as porosity, porous size, and shape including the deposition of organic-inorganic bioactive functionalized layer were successfully developed. This porous scaffold shows the promising possibility for utilizing as the alternative scaffold for bone regenerative purpose. For the further study, the in vivo study should be performed to clarify the response of the developing scaffold toward the primary bone cells under the physiological condition.

CHAPTER 3

Conclusion

In summary, the highly opened porous PLA/PBAT scaffold with well interconnected porous networks was successfully fabricated by gas foaming/ particulate leaching which applied the ammonium bicarbonate particles as the effervescent agent. This technique is simple and effective method for preparing the scaffold with three-dimensional porous architecture in various shapes. It performs in mild and facile conditions without necessarily for the special equipment.

The generation of the effervescing event due to the decomposition of ammonium bicarbonate particles when exposing to hot water leads to the formation of the porous structures in different in sizes, shape, and diameter throughout the whole piece of the scaffold. The data from present study shows that the scaffold porosity and porous diameter are in the range that suitable for bone cells to regenerate and it also suitable for oxygen and nutrients exchange as well as the formation of the new blood vessels.

The biocompatibility, bioactivity, and osteogenesis property were successfully engineered on the entire surfaces of the complicated three-dimensional porous architecture of the PLA/PBAT scaffold by PDA-assisted biomineralization technique. This simple surface modification technique has two main steps. First, the multifunctional layer with specific functional groups is developed by the simple dipping in dopamine in Tri-HCL solution. The strong and reliable deposition of the PDA multifunctional layer on the entire surface of the three-dimensional porous PLA/PBAT scaffold provides the catechol and amine functional groups as the specific sites for further chemical interaction with the other biomolecules. Second, the formation of biomineral is performed on the scaffold primed with PDA by simple dipping in $10\times$ SBF-like solution to develop the biomimetic organic-inorganic bioactive layer composed of PDA, amorphous calcium phosphate, and hydroxyapatite crystals on the surface of the PLA/PBAT scaffold.

43

The improvement on the scaffold surface hydrophilicity and the *in vitro* bioactivity as well as the *in vitro* osteogenicity toward the human-osteoblast cells line (MG-63) was observed. The formation of the surface architectures in nano and micro scale due to the deposition of the organic-inorganic bio-composites layer which composed of the plate-like apatite crystals and CaP mineral nodules on porous PLA/PBAT scaffold surface following the PDA-assisted biomineralization could play a major role on these biological improvements of the prepared scaffold. In addition, the scaffold integrity is confirmed following the in vitro biodegradation test for 30 days in PBS solution. The developing scaffold exhibits the compressible property that made it suitable for applying as the porous biomaterial for filling in the tooth extracted socket to control the dimensional shrinkage of alveolar bone following the natural tooth loss.

According to the reasons previously mentioned, the porous PLA/PBAT scaffold with PDA-assisted biomineralization exhibits the promising potential for use as a scaffold for bone regenerative purpose or the alternative biomaterial for bone tissue engineering as well as tooth socket filling biomaterial for socket preservation technique. However, the further study on immunological responses as well as the in vivo experimental research are required before the clinical applications.

44

References

Abd Alsaheb, R. A., Aladdin, A., Othman, N. Z., Abd Malek, R., Leng, O. M., Aziz, R., & El Enshasy, H. A. (2015). Recent applications of polylactic acid in pharmaceutical and medical industries. Journal of Chemical and Pharmaceutical Research, 7(12), 51-63.

Adsul, M. G., Varma, A. J., & Gokhale, D. V. (2007). Lactic acid production from waste sugarcane bagasse derived cellulose [10.1039/B605839F]. Green Chemistry, 9(1), 58-62.

Albrektsson, T., & Johansson, C. (2001). Osteoinduction, osteoconduction and osseointegration. European Spine Journal, 10 Suppl 2(Suppl 2), S96-101.

Amani, H., Arzaghi, H., Bayandori, M., Dezfuli, A. S., Pazoki-Toroudi, H., Shafiee, A., & Moradi, L. (2019). Controlling cell behavior through the design of biomaterial surfaces: a focus on surface modification techniques. Advanced materials interfaces, 6(13), 1900572.

Amini, A. R., Laurencin, C. T., & Nukavarapu, S. P. (2012). Bone tissue engineering: recent advances and challenges. Crit Rev Biomed Eng, 40(5), 363-408.

Amirazad, H., Dadashpour, M., & Zarghami, N. (2022). Application of decellularized bone matrix as a bioscaffold in bone tissue engineering. Journal of Biological Engineering, 16(1), 1.

Amler, M. H. (1969). The time sequence of tissue regeneration in human extraction wounds. Oral Surg Oral Med Oral Pathol, 27(3), 309-318.

Araújo, M., Linder, E., Wennström, J., & Lindhe, J. (2008). The influence of Bio-Oss Collagen on healing of an extraction socket: an experimental study in the dog. International Journal of Periodontics & Restorative Dentistry, 28(2).

Araújo, M. G., & Lindhe, J. (2005). Dimensional ridge alterations following tooth extraction. An experimental study in the dog. Journal of Clinical Periodontology, 32(2), 212-218.

Araújo, M. G., & Lindhe, J. (2009). Ridge preservation with the use of Bio-Oss® collagen: A 6-month study in the dog. Clinical oral implants research, 20(5), 433-440.

Arslan, A., Çakmak, S., & Gümüşderelioğlu, M. (2018). Enhanced osteogenic activity with boron-doped nanohydroxyapatite-loaded poly(butylene adipate-co-terephthalate) fibrous 3D matrix. Artif Cells Nanomed Biotechnol, 46(sup2), 790-799.

Artzi, Z., & Nemcovsky, C. E. (1998). The application of deproteinized bovine bone mineral for ridge preservation prior to implantation. Clinical and histological observations in a case report. J Periodontol, 69(9), 1062-1067.

Ashman, A. (2000a). Postextraction ridge preservation using a synthetic alloplast. Implant Dentistry, 9(2), 168-176.

Ashman, A. (2000b). Ridge preservation: important buzzwords in dentistry. General Dentistry, 48(3), 304-312.

Ashothaman, A., Sudha, J., & Senthilkumar, N. (2021). A comprehensive review on biodegradable polylactic acid polymer matrix composite material reinforced with synthetic and natural fibers. Materials Today: Proceedings.

Atwood, D. A. (1963). Postextraction changes in the adult mandible as illustrated by microradiographs of midsagittal sections and serial cephalometric roentgenograms. The Journal of Prosthetic Dentistry, 13(5), 810-824.

Baptista, R., & Guedes, M. (2021). Morphological and mechanical characterization of 3D printed PLA scaffolds with controlled porosity for trabecular bone tissue replacement. Materials Science and Engineering C, 118, 111528.

Baranwal, J., Barse, B., Fais, A., Delogu, G. L., & Kumar, A. (2022). Biopolymer: A sustainable material for food and medical applications. Polymers, 14(5), 983.

Bauer, T. W., & Muschler, G. F. (2000). Bone graft materials: an overview of the basic science. Clinical Orthopaedics and Related Research®, 371, 10-27.

Becker, W., Urist, M., Becker, B. E., Jackson, W., Parry, D. A., Bartold, M., Vincenzzi, G., De Georges, D., & Niederwanger, M. (1996). Clinical and histologic observations of sites implanted with intraoral autologous bone grafts or allografts. 15 human case reports. J Periodontol, 67(10), 1025-1033.

Bharadwaz, A., & Jayasuriya, A. C. (2020). Recent trends in the application of widely used natural and synthetic polymer nanocomposites in bone tissue regeneration. Materials Science and Engineering: C, 110, 110698.

46

Bharadwaz, A., & Jayasuriya, A. C. (2020). Recent trends in the application of widely used natural and synthetic polymer nanocomposites in bone tissue regeneration. Mater Sci Eng C Mater Biol Appl, 110, 110698.

Biswal, T. (2021). Biopolymers for tissue engineering applications: A review. Materials Today: Proceedings, 41, 397-402.

Boskey, A. L. (2007). Mineralization of bones and teeth. Elements, 3(6), 385-391.

Boyne, P. J. (1966). Osseous repair of the postextraction alveolus in man. Oral Surgery, Oral Medicine, Oral Pathology, 21(6), 805-813.

Brandam, L., Malmstrom, H., Javed, F., Calvo-Guirado, J. L., & Romanos, G. E. (2015). Ridge Preservation Techniques in the Anterior Esthetic Zone. Implant Dent, 24(6), 699-712.

Burdick, J. A., Mauck, R. L., Gorman III, J. H., & Gorman, R. C. (2013). Acellular biomaterials: an evolving alternative to cell-based therapies. Science translational medicine, 5(176), 176ps174-176ps174.

Burny, F., Donkerwolcke, M., & Muster, D. (1995). Biomaterials education: a challenge for medicine and industry in the late 1990s. Materials Science and Engineering: A, 199(1), 53-59.

Cai, Q., Xu, Q., Feng, Q., Cao, X., Yang, X., & Deng, X. (2011). Biomineralization of electrospun poly (l-lactic acid)/gelatin composite fibrous scaffold by using a supersaturated simulated body fluid with continuous CO_2 bubbling. Applied Surface Science, 257(23), 10109-10118.

Cardaropoli, G., Araújo, M., & Lindhe, J. (2003). Dynamics of bone tissue formation in tooth extraction sites. An experimental study in dogs. J Clin Periodontol, 30(9), 809-818.

Chen, X., Li, Y., & Hodgson, P. D. (2009). Microstructures and bond strengths of the calcium phosphate coatings formed on titanium from different simulated body fluids. Materials Science and Engineering: C, 29(1), 165-171.

Chen, X., Zhu, L., Liu, H., Wen, W., Li, H., Zhou, C., & Luo, B. (2019). Biomineralization guided by polydopamine-modifed poly (L-lactide) fibrous membrane for promoted osteoconductive activity. Biomedical Materials, 14(5), 055005.

47

Cheng, Y., Deng, S., Chen, P., & Ruan, R. (2009). Polylactic acid (PLA) synthesis and modifications: a review. Frontiers of chemistry in China, 4(3), 259-264.

Chocholata, P., Kulda, V., & Babuska, V. (2019). Fabrication of scaffolds for bone-tissue regeneration. Materials, 12(4), 568.

Christensen, G. J. (1996). Ridge preservation: why not? J Am Dent Assoc, 127(5), 669-670.

Corral, D. A., Amling, M., Priemel, M., Loyer, E., Fuchs, S., Ducy, P., Baron, R., & Karsenty, G. (1998). Dissociation between bone resorption and bone formation in osteopenic transgenic mice. Proceedings of the National Academy of Sciences, 95(23), 13835-13840.

Cui, J., Ma, C., Li, Z., Wu, L., Wei, W., Chen, M., Peng, B., & Deng, Z. (2016). Polydopamine-functionalized polymer particles as templates for mineralization of hydroxyapatite: biomimetic and in vitro bioactivity. RSC Advances, 6(8), 6747-6755.

Da Silva, D., Kaduri, M., Poley, M., Adir, O., Krinsky, N., Shainsky-Roitman, J., & Schroeder, A. (2018). Biocompatibility, biodegradation and excretion of polylactic acid (PLA) in medical implants and theranostic systems. Chemical Engineering Journal, 340, 9-14.

Deng, Y., Yang, W.-Z., Shi, D., Wu, M., Xiong, X.-L., Chen, Z.-G., & Wei, S.-C. (2019). Bioinspired and osteopromotive polydopamine nanoparticle-incorporated fibrous membranes for robust bone regeneration. NPG Asia Materials, 11(1), 39.

DeStefano, V., Khan, S., & Tabada, A. (2020). Applications of PLA in modern medicine. Engineered Regeneration, 1, 76-87.

Devlin, H., & Sloan, P. (2002). Early bone healing events in the human extraction socket. International journal of oral and maxillofacial surgery, 31(6), 641-645.

Dorozhkin, S. V. (2013). A detailed history of calcium orthophosphates from 1770s till 1950. Materials Science and Engineering: C, 33(6), 3085-3110.

Draenert, F. G., Kämmerer, P. W., Berthold, M., & Neff, A. (2016). Complications with allogeneic, cancellous bone blocks in vertical alveolar ridge augmentation: prospective clinical case study and review of the literature. Oral Surg Oral Med Oral Pathol Oral Radiol, 122(2), e31-43.

48

Du, J., Zhou, Y., Bao, X., Kang, Z., Huang, J., Xu, G., Yi, C., & Li, D. (2022). Surface polydopamine modification of bone defect repair materials: Characteristics and applications [Review]. Frontiers in bioengineering and biotechnology, 10.

Farah, S., Anderson, D. G., & Langer, R. (2016). Physical and mechanical properties of PLA, and their functions in widespread applications — A comprehensive review. Advanced Drug Delivery Reviews, 107, 367-392.

Farmer, M., & Darby, I. (2014). Ridge dimensional changes following single-tooth extraction in the aesthetic zone. Clin Oral Implants Res, 25(2), 272-277.

Fedorovich, N. E., Alblas, J., Hennink, W. E., Öner, F. C., & Dhert, W. J. A. (2011). Organ printing: the future of bone regeneration? Trends in Biotechnology, 29(12), 601-606.

Ferrari, M., Cirisano, F., & Morán, M. C. (2019). Mammalian cell behavior on hydrophobic substrates: influence of surface properties. Colloids and Interfaces, 3(2), 48.

Ferreira, F. V., Cividanes, L. S., Gouveia, R. F., & Lona, L. M. (2019). An overview on properties and applications of poly (butylene adipate-co-terephthalate)–PBAT based composites. Polymer Engineering & Science, 59(s2), E7-E15.

Fickl, S., Zuhr, O., Wachtel, H., Bolz, W., & Huerzeler, M. (2008). Tissue alterations after tooth extraction with and without surgical trauma: a volumetric study in the beagle dog. J Clin Periodontol, 35(4), 356-363.

Froum, S., Cho, S. C., Rosenberg, E., Rohrer, M., & Tarnow, D. (2002). Histological comparison of healing extraction sockets implanted with bioactive glass or demineralized freeze-dried bone allograft: a pilot study. J Periodontol, 73(1), 94-102.

Fukushima, K., & Kimura, Y. (2008). An efficient solid-state polycondensation method for synthesizing stereocomplexed poly (lactic acid) s with high molecular weight. Journal of Polymer Science Part A: Polymer Chemistry, 46(11), 3714-3722.

Fukushima, K., Wu, M.-H., Bocchini, S., Rasyida, A., & Yang, M.-C. (2012). PBAT based nanocomposites for medical and industrial applications. Materials Science and Engineering: C, 32(6), 1331-1351.

49

Gao, C., Peng, S., Feng, P., & Shuai, C. (2017). Bone biomaterials and interactions with stem cells. Bone Research, 5(1), 1-33.

Garavand, F., Rouhi, M., Razavi, S. H., Cacciotti, I., & Mohammadi, R. (2017). Improving the integrity of natural biopolymer films used in food packaging by crosslinking approach: A review. International journal of biological macromolecules, 104, 687-707.

Garetto, L. P., Chen, J., Parr, J. A., & Roberts, W. E. (1995). Remodeling dynamics of bone supporting rigidly fixed titanium implants: a histomorphometric comparison in four species including humans. Implant Dentistry, 4(4), 235-243.

Ghassemi, T., Shahroodi, A., Ebrahimzadeh, M. H., Mousavian, A., Movaffagh, J., & Moradi, A. (2018). Current concepts in scaffolding for bone tissue engineering. Archives of bone and joint surgery, 6(2), 90.

Ghorbani, F., Zamanian, A., Behnamghader, A., & Daliri-Joupari, M. (2019). Bone-like hydroxyapatite mineralization on the bio-inspired PDA nanoparticles using microwave irradiation. Surfaces and Interfaces, 15, 38-42.

Ghorbani, F., Zamanian, A., Behnamghader, A., & Joupari, M. D. (2019). A facile method to synthesize mussel-inspired polydopamine nanospheres as an active template for in situ formation of biomimetic hydroxyapatite. Materials Science and Engineering: C, 94, 729-739.

Gittens, R. A., McLachlan, T., Olivares-Navarrete, R., Cai, Y., Berner, S., Tannenbaum, R., Schwartz, Z., Sandhage, K. H., & Boyan, B. D. (2011). The effects of combined micron-/submicron-scale surface roughness and nanoscale features on cell proliferation and differentiation. Biomaterials, 32(13), 3395-3403.

Gopferich, A. (1997). Erosion of composite polymer matrices. Biomaterials, 18(5), 397-403.

Green, D., Howard, D., Yang, X., Kelly, M., & Oreffo, R. (2003). Natural marine sponge fiber skeleton: a biomimetic scaffold for human osteoprogenitor cell attachment, growth, and differentiation. Tissue engineering, 9(6), 1159-1166.

Guglielmotti, M. B., & Cabrini, R. L. (1985). Alveolar wound healing and ridge remodeling after tooth extraction in the rat: A histologic, radiographic, and histometric study. Journal of Oral and Maxillofacial Surgery, 43(5), 359-364.

Hauschka, P., Mavrakos, A., Iafrati, M., Doleman, S., & Klagsbrun, M. (1986). Growth factors in bone matrix. Isolation of multiple types by affinity chromatography on heparin-Sepharose. Journal of Biological Chemistry, 261(27), 12665-12674.

Heberer, S., Al-Chawaf, B., Hildebrand, D., Nelson, J. J., & Nelson, K. (2008). Histomorphometric analysis of extraction sockets augmented with Bio-Oss Collagen after a 6-week healing period: a prospective study. Clin Oral Implants Res, 19(12), 1219-1225.

Ho, C. C., & Ding, S. J. (2014). Structure, properties and applications of mussel-inspired polydopamine. J Biomed Nanotechnol, 10(10), 3063-3084.

Huo, Y., Lu, Y., Meng, L., Wu, J., Gong, T., Zou, J. a., Bosiakov, S., & Cheng, L. (2021). A Critical Review on the Design, Manufacturing and Assessment of the Bone Scaffold for Large Bone Defects [Review]. Frontiers in bioengineering and biotechnology, 9.

Hutmacher, D. W. (2000). Scaffolds in tissue engineering bone and cartilage. Biomaterials, 21(24), 2529-2543.

Hutmacher, D. W., Schantz, J. T., Lam, C. X., Tan, K. C., & Lim, T. C. (2007). State of the art and future directions of scaffold-based bone engineering from a biomaterials perspective. Journal of Tissue Engineering and Regenerative Medicine, 1(4), 245-260.

Idaszek, J., Zinn, M., Obarzanek-Fojt, M., Zell, V., Swieszkowski, W., & Bruinink, A. (2013). Tailored degradation of biocompatible poly(3-hydroxybutyrate-co-3-hydroxyvalerate)/calcium silicate/poly(lactide-co-glycolide) ternary composites: An in vitro study. Materials Science and Engineering: C, 33(7), 4352-4360.

Inkinen, S., Hakkarainen, M., Albertsson, A.-C., & Södergård, A. (2011). From Lactic Acid to Poly(lactic acid) (PLA): Characterization and Analysis of PLA and Its Precursors. Biomacromolecules, 12(3), 523-532.

Iqbal, N., Khan, A. S., Asif, A., Yar, M., Haycock, J. W., & Rehman, I. U. (2019). Recent concepts in biodegradable polymers for tissue engineering paradigms: A critical review. International Materials Reviews, 64(2), 91-126.

Januário, A. L., Duarte, W. R., Barriviera, M., Mesti, J. C., Araújo, M. G., & Lindhe, J. (2011). Dimension of the facial bone wall in the anterior maxilla: a cone-beam computed tomography study. Clinical oral implants research, 22(10), 1168-1171.

Jia, L., Han, F., Wang, H., Zhu, C., Guo, Q., Li, J., Zhao, Z., Zhang, Q., Zhu, X., & Li, B. (2019). Polydopamine-assisted surface modification for orthopaedic implants. Journal of orthopaedic translation, 17, 82-95.

Kang, Y., Chen, P., Shi, X., Zhang, G., & Wang, C. (2018). Preparation of open-porous stereocomplex PLA/PBAT scaffolds and correlation between their morphology, mechanical behavior, and cell compatibility. RSC advances, 8(23), 12933-12943.

Kaushik, N., Nhat Nguyen, L., Kim, J. H., Choi, E. H., & Kumar Kaushik, N. (2020). Strategies for using polydopamine to induce biomineralization of hydroxyapatite on implant materials for bone tissue engineering. International Journal of Molecular Sciences, 21(18), 6544.

Khatsee, S., Daranarong, D., Punyodom, W., & Worajittiphon, P. (2018). Electrospinning polymer blend of PLA and PBAT: Electrospinnability–solubility map and effect of polymer solution parameters toward application as antibiotic-carrier mats. Journal of applied polymer science, 135(28), 46486.

Ko, E., Lee, J. S., Kim, H., Yang, S. Y., Yang, D., Yang, K., Lee, J., Shin, J., Yang, H. S., & Ryu, W. (2017). Electrospun silk fibroin nanofibrous scaffolds with two-stage hydroxyapatite functionalization for enhancing the osteogenic differentiation of human adipose-derived mesenchymal stem cells. ACS Applied Materials & Interfaces, 10(9), 7614-7625.

Kohane, D. S., & Langer, R. (2008). Polymeric biomaterials in tissue engineering. Pediatric Research, 63(5), 487-491.

Kokubo, T., Kushitani, H., Sakka, S., Kitsugi, T., & Yamamuro, T. (1990). Solutions able to reproduce in vivo surface-structure changes in bioactive glass-ceramic A-W3. Journal of Biomedical Materials Research, 24(6), 721-734.

Kokubo, T., & Takadama, H. (2006). How useful is SBF in predicting in vivo bone bioactivity? Biomaterials, 27(15), 2907-2915.

Kolk, A., Handschel, J., Drescher, W., Rothamel, D., Kloss, F., Blessmann, M., Heiland, M., Wolff, K. D., & Smeets, R. (2012). Current trends and future perspectives of

bone substitute materials - from space holders to innovative biomaterials. Journal of Cranio-Maxillofacial Surgery, 40(8), 706-718.

Kondratowicz, F. Ł., & Ukielski, R. (2009). Synthesis and hydrolytic degradation of poly(ethylene succinate) and poly(ethylene terephthalate) copolymers. Polymer Degradation and Stability, 94(3), 375-382.

Kular, J., Tickner, J., Chim, S. M., & Xu, J. (2012). An overview of the regulation of bone remodelling at the cellular level. Clinical biochemistry, 45(12), 863-873.

Kulkarni, R., Pani, K., Neuman, C., & Leonard, F. (1966). Polylactic acid for surgical implants. Archives of surgery, 93(5), 839-843.

Kumar, P., Vinitha, B., & Fathima, G. (2013). Bone grafts in dentistry. Journal of pharmacy & bioallied sciences, 5(Suppl 1), S125.

Langer, R., & Vacanti, J. P. (1993). Tissue engineering. Science, 260(5110), 920-926.

Lasprilla, A. J. R., Martinez, G. A. R., Lunelli, B. H., Jardini, A. L., & Filho, R. M. (2012). Poly-lactic acid synthesis for application in biomedical devices — A review. Biotechnology Advances, 30(1), 321-328.

Latimer, J. M., Maekawa, S., Yao, Y., Wu, D. T., Chen, M., & Giannobile, W. V. (2021). Regenerative medicine technologies to treat dental, oral, and craniofacial defects. Frontiers in bioengineering and biotechnology, 637.

Le, B. Q., Nurcombe, V., Cool, S. M., van Blitterswijk, C. A., de Boer, J., & LaPointe, V. L. S. (2017). The Components of Bone and What They Can Teach Us about Regeneration. Materials (Basel), 11(1).

Lee, H., Dellatore, S. M., Miller, W. M., & Messersmith, P. B. (2007). Mussel-inspired surface chemistry for multifunctional coatings. Science, 318(5849), 426-430.

Lee, H., Dellatore, S. M., Miller, W. M., & Messersmith, P. B. (2007). Mussel-inspired surface chemistry for multifunctional coatings. Science, 318(5849), 426-430.

LeGeros, R. Z. (2008). Calcium phosphate-based osteoinductive materials. Chemical reviews, 108(11), 4742-4753.

Lei, B., Guo, B., Rambhia, K. J., & Ma, P. X. (2019). Hybrid polymer biomaterials for bone tissue regeneration. Frontiers in Medicine, 13(2), 189-201.

Lekovic, V., Camargo, P. M., Klokkevold, P. R., Weinlaender, M., Kenney, E. B., Dimitrijevic, B., & Nedic, M. (1998). Preservation of alveolar bone in extraction

sockets using bioabsorbable membranes. Journal of Clinical Periodontology, 69(9), 1044-1049.

Lekovic, V., Kenney, E. B., Weinlaender, M., Han, T., Klokkevold, P., Nedic, M., & Orsini, M. (1997). A bone regenerative approach to alveolar ridge maintenance following tooth extraction. Report of 10 cases. Journal of Periodontology, 68(6), 563-570.

Lim, L. T., Auras, R., & Rubino, M. (2008). Processing technologies for poly(lactic acid). Progress in Polymer Science, 33(8), 820-852.

Limmahakhun, S., Oloyede, A., Sitthiseripratip, K., Xiao, Y., & Yan, C. (2017). 3D-printed cellular structures for bone biomimetic implants. Additive Manufacturing, 15, 93-101.

Liu, C., Li, Y., Wang, J., Liu, C., Liu, W., & Jian, X. (2018). Improving Hydrophilicity and Inducing Bone-Like Apatite Formation on PPBES by Polydopamine Coating for Biomedical Application. Molecules, 23(7), 1643.

Liu, S., Qin, S., He, M., Zhou, D., Qin, Q., & Wang, H. (2020). Current applications of poly (lactic acid) composites in tissue engineering and drug delivery. Composites Part B: Engineering, 199, 108238.

Liu, Y., Yang, L., Chen, G., Liu, Z., Lu, T., Yang, Y., Yu, J., Kang, D., Yan, W., He, M., Qin, S., Yu, J., Ye, C., & Luo, H. (2021). PBAT hollow porous microfibers prepared via electrospinning and their functionalization for potential peptide release. Materials & Design, 207, 109880.

Lloyd, A. W. (2002). Interfacial bioengineering to enhance surface biocompatibility. Medical device technology, 13(1), 18-21.

Lynge, M. E., van der Westen, R., Postma, A., & Städler, B. (2011). Polydopamine—a nature-inspired polymer coating for biomedical science [10.1039/C1NR10969C]. Nanoscale, 3(12), 4916-4928.

Maia-Pinto, M. O., Brochado, A. C. B., Teixeira, B. N., Sartoretto, S. C., Uzeda, M. J., Alves, A. T., Alves, G. G., Calasans-Maia, M. D., & Thiré, R. M. (2020). Biomimetic mineralization on 3D printed PLA scaffolds: on the response of human primary osteoblasts spheroids and in vivo implantation. Polymers, 13(1), 74.

Masaki, C., Nakamoto, T., Mukaibo, T., Kondo, Y., & Hosokawa, R. (2015). Strategies for alveolar ridge reconstruction and preservation for implant therapy. J Prosthodont Res, 59(4), 220-228.

Mercado-Pagan, A. E., Stahl, A. M., Shanjani, Y., & Yang, Y. (2015). Vascularization in bone tissue engineering constructs. Ann Biomed Eng, 43(3), 718-729.

Migliaresi, C., De Lollis, A., Fambri, L., & Cohn, D. (1991). The effect of thermal history on the crystallinity of different molecular weight PLLA biodegradable polymers. Clinical Materials, 8(1), 111-118.

Mohapatra, A. K., Mohanty, S., & Nayak, S. K. (2014). Effect of PEG on PLA/PEG blend and its nanocomposites: A study of thermo-mechanical and morphological characterization. Polymer Composites, 35(2), 283-293.

Moustafa, H., El Kissi, N., Abou-Kandil, A. I., Abdel-Aziz, M. S., & Dufresne, A. (2017). PLA/PBAT Bionanocomposites with Antimicrobial Natural Rosin for Green Packaging. ACS Applied Materials & Interfaces, 9(23), 20132-20141.

Murari, G., Bock, N., Zhou, H., Yang, L., Liew, T., Fox, K., & Tran, P. A. (2020). Effects of polydopamine coatings on nucleation modes of surface mineralization from simulated body fluid. Scientific Reports, 10(1), 14982.

Nair, L. S., & Laurencin, C. T. (2006). Polymers as biomaterials for tissue engineering and controlled drug delivery. Tissue engineering I, 47-90.

Nair, L. S., & Laurencin, C. T. (2007). Biodegradable polymers as biomaterials. Progress in polymer science, 32(8-9), 762-798.

Nampoothiri, K. M., Nair, N. R., & John, R. P. (2010). An overview of the recent developments in polylactide (PLA) research. Bioresource technology, 101(22), 8493-8501.

Nicklisch, S., & Waite, J. (2012). Mini-review: The role of redox in DOPA-mediated marine adhesion. Biofouling, 28, 865-877.

Nofar, M., Sacligil, D., Carreau, P. J., Kamal, M. R., & Heuzey, M.-C. (2019). Poly (lactic acid) blends: Processing, properties and applications. International journal of biological macromolecules, 125, 307-360.

Nofar, M., Tabatabaei, A., Sojoudiasli, H., Park, C., Carreau, P., Heuzey, M.-C., & Kamal, M. (2017). Mechanical and bead foaming behavior of PLA-PBAT and

PLA-PBSA blends with different morphologies. European Polymer Journal, 90, 231-244.

Nothling, M. D., Bailey, C. G., Fillbrook, L. L., Wang, G., Gao, Y., McCamey, D. R., Monfared, M., Wong, S., Beves, J. E., & Stenzel, M. H. (2022). Polymer Grafting to Polydopamine Free Radicals for Universal Surface Functionalization. Journal of the American Chemical Society, 144(15), 6992-7000.

Nyamweya, N. N. (2021). Applications of polymer blends in drug delivery. Future Journal of Pharmaceutical Sciences, 7, 1-15.

Ohtsuki, C., Kamitakahara, M., & Miyazaki, T. (2007). Coating bone-like apatite onto organic substrates using solutions mimicking body fluid. Journal of Tissue Engineering and Regenerative Medicine, 1(1), 33-38.

Okada, M. (2002). Chemical syntheses of biodegradable polymers. Progress in Polymer Science, 27(1), 87-133.

Olewnik, E., & Czerwiński, W. (2009). Synthesis, structural study and hydrolytic degradation of copolymer based on glycolic acid and bis-2-hydroxyethyl terephthalate. Polymer Degradation and Stability, 94(2), 221-226.

Palmer, L. C., Newcomb, C. J., Kaltz, S. R., Spoerke, E. D., & Stupp, S. I. (2008). Biomimetic systems for hydroxyapatite mineralization inspired by bone and enamel. Chemical reviews, 108(11), 4754-4783.

Pang, X., Zhuang, X., Tang, Z., & Chen, X. (2010). Polylactic acid (PLA): Research, development and industrialization. Biotechnology Journal, 5(11), 1125-1136.

Papadimitriou, D. E., Chochlidakis, K. M., Weitz, D. S., Wazirian, B., & Ercoli, C. (2014). Surgical and prosthetic management of ridge deficiency for an implant-supported restoration in the esthetic zone. J Prosthet Dent, 112(3), 409-413.

Park, J., Lee, S. J., Jung, T. G., Lee, J. H., Kim, W. D., Lee, J. Y., & Park, S. A. (2021). Surface modification of a three-dimensional polycaprolactone scaffold by polydopamine, biomineralization, and BMP-2 immobilization for potential bone tissue applications. Colloids and Surfaces B: Biointerfaces, 199, 111528.

Patra, D., & Seeger, S. (2017). Hydroxyapatite biomineralization on functionalized silicone nanofilaments. Colloid and Interface Science Communications, 16, 1-5.

Paul, D., & Barlow, J. (1980). Polymer blends. Journal of Macromolecular Science— Reviews in Macromolecular Chemistry, 18(1), 109-168.

Perego, G., Cella, G. D., & Bastioli, C. (1996). Effect of molecular weight and crystallinity on poly(lactic acid) mechanical properties [Article]. Journal of Applied Polymer Science, 59(1), 37-43.

Pietrokovski, J., & Massler, M. (1967). Alveolar ridge resorption following tooth extraction. Journal of Prosthetic Dentistry, 17(1), 21-27.

Pietrosanto, A., Scarfato, P., Di Maio, L., Nobile, M. R., & Incarnato, L. (2020). Evaluation of the suitability of poly (lactide)/poly (butylene-adipate-co-terephthalate) blown films for chilled and frozen food packaging applications. Polymers, 12(4), 804.

Place, E. S., George, J. H., Williams, C. K., & Stevens, M. M. (2009). Synthetic polymer scaffolds for tissue engineering. Chemical Society Reviews, 38(4), 1139-1151.

Polo-Corrales, L., Latorre-Esteves, M., & Ramirez-Vick, J. E. (2014). Scaffold design for bone regeneration. Journal of nanoscience and nanotechnology, 14(1), 15-56.

Reichert, J. C., Wullschleger, M. E., Cipitria, A., Lienau, J., Cheng, T. K., Schutz, M. A., Duda, G. N., Noth, U., Eulert, J., & Hutmacher, D. W. (2011). Custom-made composite scaffolds for segmental defect repair in long bones. Int Orthop, 35(8), 1229-1236.

Rho, J.-Y., Kuhn-Spearing, L., & Zioupos, P. (1998). Mechanical properties and the hierarchical structure of bone. Medical Engineering and Physics, 20(2), 92-102.

Riau, A. K., Venkatraman, S. S., & Mehta, J. S. (2020). Biomimetic vs. direct approach to deposit hydroxyapatite on the surface of low melting point polymers for tissue engineering. Nanomaterials, 10(11), 2162.

Ryu, J., Ku, S. H., Lee, H., & Park, C. B. (2010). Mussel-inspired polydopamine coating as a universal route to hydroxyapatite crystallization. Advanced Functional Materials, 20(13), 2132-2139.

Saini, P., Arora, M., & Kumar, M. R. (2016). Poly (lactic acid) blends in biomedical applications. Advanced Drug Delivery Reviews, 107, 47-59.

Sarasua, J. R., Arraiza, A. L., Balerdi, P., & Maiza, I. (2005). Crystallinity and mechanical properties of optically pure polylactides and their blends [Article]. Polymer Engineering and Science, 45(5), 745-753.

Schropp, L., Wenzel, A., Kostopoulos, L., & Karring, T. (2003). Bone healing and soft tissue contour changes following single-tooth extraction: a clinical and radiographic 12-month prospective study. International Journal of Periodontics and Restorative Dentistry, 23(4), 313-323.

Shin, K., Acri, T., Geary, S., & Salem, A. K. (2017). Biomimetic mineralization of biomaterials using simulated body fluids for bone tissue engineering and regenerative medicine. Tissue Engineering Part A, 23(19-20), 1169-1180.

Shin, M., Yoon, T., Yang, B., & Cha, H. J. (2022). Thiol-Rich fp-6 Controls the Tautomer Equilibrium of Oxidized Dopa in Interfacial Mussel Foot Proteins. Langmuir, 38(11), 3446-3452.

Simpson, H. E. (1969). The healing of extraction wounds. British Dental Journal, 126(12), 550-557.

Skalak, R., & Fox, C. F. (1988). *Tissue engineering: proceedings of a workshop, held at Granlibakken, Lake Tahoe, California, February 26-29, 1988* (Vol. 107). Alan R. Liss.

Song, R., Murphy, M., Li, C., Ting, K., Soo, C., & Zheng, Z. (2018). Current development of biodegradable polymeric materials for biomedical applications. Drug Design, Development and Therapy, 12, 3117-3145.

Soni, R. K., Soam, S., & Dutt, K. (2009). Studies on biodegradability of copolymers of lactic acid, terephthalic acid and ethylene glycol. Polymer Degradation and Stability, 94(3), 432-437.

Su, S., Duhme, M., & Kopitzky, R. (2020). Uncompatibilized PBAT/PLA blends: manufacturability, miscibility and properties. Materials, 13(21), 4897.

Su, S., Duhme, M., & Kopitzky, R. (2020). Uncompatibilized PBAT/PLA Blends: Manufacturability, Miscibility and Properties. Materials (Basel), 13(21).

Surmenev, R. A., Surmeneva, M. A., & Ivanova, A. A. (2014). Significance of calcium phosphate coatings for the enhancement of new bone osteogenesis–a review. Acta Biomaterialia, 10(2), 557-579.

58

Taib, N.-A. A. B., Rahman, M. R., Huda, D., Kuok, K. K., Hamdan, S., Bakri, M. K. B., Julaihi, M. R. M. B., & Khan, A. (2022). A review on poly lactic acid (PLA) as a biodegradable polymer. Polymer Bulletin, 1-35.

Tajbakhsh, S., & Hajiali, F. (2017). A comprehensive study on the fabrication and properties of biocomposites of poly (lactic acid)/ceramics for bone tissue engineering. Materials Science and Engineering: C, 70, 897-912.

Tanahashi, M., & Matsuda, T. (1997). Surface functional group dependence on apatite formation on self-assembled monolayers in a simulated body fluid. Journal of Biomedical Materials Research: An Official Journal of The Society for Biomaterials and The Japanese Society for Biomaterials, 34(3), 305-315.

Tanahashi, M., Yao, T., Kokubo, T., Minoda, M., Miyamoto, T., Nakamura, T., & Yamamuro, T. (1994). Apatite coating on organic polymers by a biomimetic process. Journal of the American Ceramic Society, 77(11), 2805-2808.

Tang, Z., Li, X., Tan, Y., Fan, H., & Zhang, X. (2018). The material and biological characteristics of osteoinductive calcium phosphate ceramics. Regenerative biomaterials, 5(1), 43-59.

Tas, A. C., & Bhaduri, S. B. (2004). Rapid coating of Ti6Al4V at room temperature with a calcium phosphate solution similar to $10\times$ simulated body fluid. Journal of Materials Research, 19(9), 2742-2749.

Teixeira, S., Eblagon, K. M., Miranda, F., R. Pereira, M. F., & Figueiredo, J. L. (2021). Towards Controlled Degradation of Poly(lactic) Acid in Technical Applications. C, 7(2), 42.

Tipduangta, P., Belton, P., McAuley, W. J., & Qi, S. (2021). The use of polymer blends to improve stability and performance of electrospun solid dispersions: The role of miscibility and phase separation. International Journal of Pharmaceutics 602, 120637.

Toh, H. W., Toong, D. W. Y., Ng, J. C. K., Ow, V., Lu, S., Tan, L. P., Wong, P. E. H., Venkatraman, S., Huang, Y., & Ang, H. Y. (2021). Polymer blends and polymer composites for cardiovascular implants. European Polymer Journal, 146, 110249.

59

Tran, P. H. L., Duan, W., Lee, B. J., & Tran, T. T. D. (2018). Current Designs of Polymer Blends in Solid Dispersions for Improving Drug Bioavailability. Current Drug Metabolism, 19(13), 1111-1118.

Trombelli, L., Farina, R., Marzola, A., Bozzi, L., Liljenberg, B., & Lindhe, J. (2008). Modeling and remodeling of human extraction sockets. Journal of Clinical Periodontology, 35(7), 630-639.

Wan, C., & Chen, B. (2011). Poly (ε-caprolactone)/graphene oxide biocomposites: mechanical properties and bioactivity. Biomedical Materials, 6(5), 055010.

Wang, J., Wang, Y., & Wu, Q. (2021). Poly (dopamine)-assisted bioactive coating on the surface of porous poly (ether ether ketone) to promote osteogenic differentiation of rBMSC. Journal of Wuhan University of Technology-Mater. Sci. Ed., 36(5), 766-776.

Wei, P., Yuan, Z., Jing, W., Huang, Y., Cai, Q., Guan, B., Liu, Z., Zhang, X., Mao, J., Chen, D., & Yang, X. (2019). Strengthening the potential of biomineralized microspheres in enhancing osteogenesis via incorporating alendronate. Chemical Engineering Journal, 368, 577-588.

Wei, W., Yu, J., Gebbie, M. A., Tan, Y., Martinez Rodriguez, N. R., Israelachvili, J. N., & Waite, J. H. (2015). Bridging adhesion of mussel-inspired peptides: Role of charge, chain length, and surface type. Langmuir, 31(3), 1105-1112.

Weng, J., Liu, Q., Wolke, J., Zhang, X., & De Groot, K. (1997). Formation and characteristics of the apatite layer on plasma-sprayed hydroxyapatite coatings in simulated body fluid. Biomaterials, 18(15), 1027-1035.

Wieszczycka, K., Staszak, K., Woźniak-Budych, M. J., Litowczenko, J., Maciejewska, B. M., & Jurga, S. (2021). Surface functionalization–The way for advanced applications of smart materials. Coordination Chemistry Reviews, 436, 213846.

Wu, S., Liu, X., Yeung, K. W. K., Liu, C., & Yang, X. (2014). Biomimetic porous scaffolds for bone tissue engineering. Materials Science and Engineering: R: Reports, 80, 1-36.

Xiao, D., Zhang, J., Zhang, C., Barbieri, D., Yuan, H., Moroni, L., & Feng, G. (2020). The role of calcium phosphate surface structure in osteogenesis and the mechanisms involved. Acta Biomaterialia, 106, 22-33.

Xie, C., Lu, X., Han, L., Xu, J., Wang, Z., Jiang, L., Wang, K., Zhang, H., Ren, F., & Tang, Y. (2016). Biomimetic mineralized hierarchical graphene oxide/chitosan scaffolds with adsorbability for immobilization of nanoparticles for biomedical applications. ACS applied materials & interfaces, 8(3), 1707-1717.

Xu, C., Xia, Y., Wang, L., Nan, X., Hou, J., Guo, Y., Meng, K., Lian, J., Zhang, Y., Wu, F., & Zhao, B. (2021). Polydopamine-assisted immobilization of silk fibroin and its derived peptide on chemically oxidized titanium to enhance biological activity in vitro. International journal of biological macromolecules, 185, 1022-1035.

Xu, L., Crawford, K., & Gorman, C. B. (2011). Effects of temperature and pH on the degradation of poly (lactic acid) brushes. Macromolecules, 44(12), 4777-4782.

Yan, D., Wang, Z., Guo, Z., Ma, Y., Wang, C., Tan, H., & Zhang, Y. (2020). Study on the properties of PLA/PBAT composite modified by nanohydroxyapatite. Journal of Materials Research and Technology, 9(5), 11895-11904.

Yan, J., Wu, R., Liao, S., Jiang, M., & Qian, Y. (2020). Applications of Polydopamine-Modified Scaffolds in the Peripheral Nerve Tissue Engineering. Front Bioeng Biotechnol, 8, 590998.

Young, M. F. (2003). Bone matrix proteins: their function, regulation, and relationship to osteoporosis. Osteoporos Int, 14 Suppl 3, S35-42.

Yu, L., Dean, K., & Li, L. (2006). Polymer blends and composites from renewable resources. Progress in polymer science, 31(6), 576-602.

Yu, X., Tang, X., Gohil, S. V., & Laurencin, C. T. (2015). Biomaterials for bone regenerative engineering. Advanced healthcare materials, 4(9), 1268-1285.

Zangmeister, R. A., Morris, T. A., & Tarlov, M. J. (2013). Characterization of Polydopamine Thin Films Deposited at Short Times by Autoxidation of Dopamine. Langmuir, 29(27), 8619-8628.

Zarrinbakhsh, N., Mohanty, A. K., & Misra, M. (2013). Improving the interfacial adhesion in a new renewable resource-based biocomposites from biofuel coproduct and biodegradable plastic. Journal of Materials Science, 48(17), 6025-6038.

Zhang, R., Lan, W., Ding, J., Ahmed, S., Qin, W., He, L., & Liu, Y. (2019). Effect of PLA/PBAT antibacterial film on storage quality of passion fruit during the shelf-life. Molecules, 24(18), 3378.

Zhao, R., Yang, R., Cooper, P. R., Khurshid, Z., Shavandi, A., & Ratnayake, J. (2021). Bone grafts and substitutes in dentistry: A review of current trends and developments. Molecules, 26(10), 3007.

Zhu, T., Cui, Y., Zhang, M., Zhao, D., Liu, G., & Ding, J. (2020). Engineered three-dimensional scaffolds for enhanced bone regeneration in osteonecrosis. Bioactive materials, 5(3), 584-601.
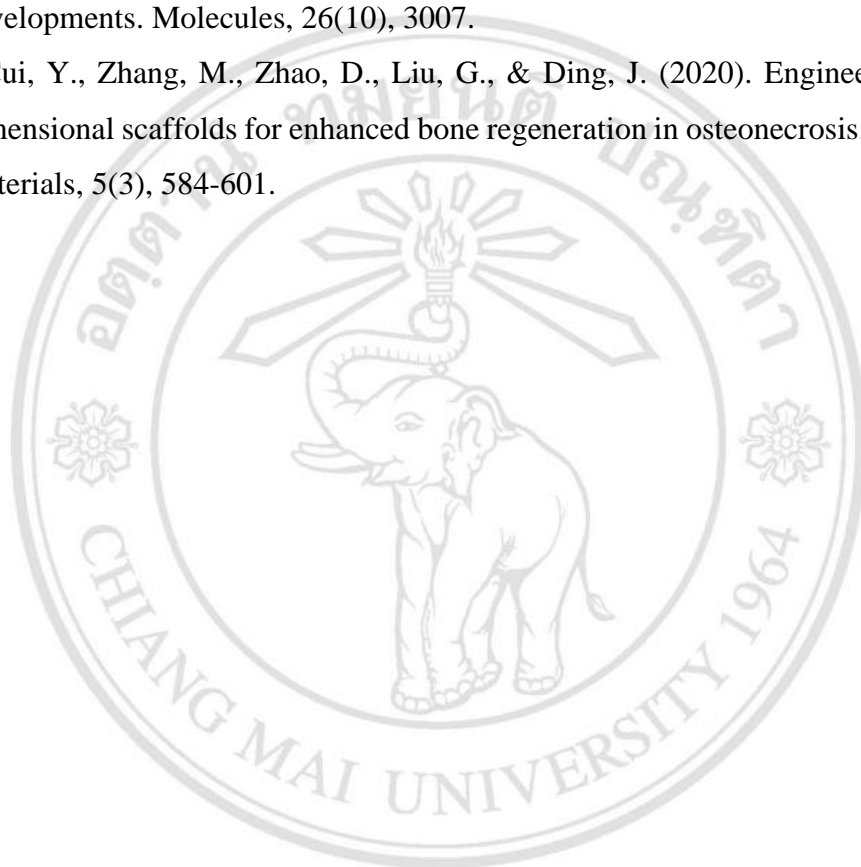
Appendix A

(Raw data and statistical analysis for the first publication)

Table A-1. The data of material degradation following the *in vitro* degration test in PBS at 7, 30, 60, and 90 days.

| | No. | 7days | | | 30days | | | 60days | | | 90days | | |
		before	after	change	before	after	change	before	after	change	before	after	change
PLA	1	0.011	0.011	1.770	0.014	0.013	4.965	0.011	0.011	4.545	0.013	0.012	3.937
	2	0.013	0.012	3.150	0.012	0.012	3.306	0.011	0.011	3.509	0.011	0.011	5.310
	3	0.009	0.008	2.326	0.013	0.013	2.308	0.013	0.012	3.150	0.010	0.010	4.950
	4	0.011	0.010	4.587	0.015	0.014	3.401	0.012	0.011	4.348	0.011	0.011	3.540
	5	0.012	0.012	2.419	0.011	0.011	3.604	0.014	0.014	2.857	0.012	0.011	5.172
	6	0.012	0.011	3.419	0.011	0.011	3.540	0.009	0.009	6.452	0.013	0.013	3.008
PLA/PEG	1	0.013	0.013	5.224	0.013	0.012	4.651	0.013	0.012	5.344	0.014	0.013	7.246
	2	0.012	0.011	6.838	0.015	0.014	6.579	0.013	0.012	5.344	0.015	0.014	5.263
	3	0.013	0.012	3.125	0.014	0.013	5.036	0.015	0.014	6.897	0.013	0.012	6.400
	4	0.013	0.013	6.015	0.012	0.012	5.691	0.013	0.012	4.688	0.014	0.013	6.569
	5	0.013	0.012	4.800	0.012	0.011	5.217	0.015	0.014	7.383	0.014	0.013	4.444
	6	0.015	0.014	5.921	0.015	0.014	5.960	0.015	0.014	5.298	0.016	0.015	5.521
PLA/PEG/5% bone dECM	1	0.014	0.013	6.569	0.015	0.014	6.803	0.014	0.013	5.755	0.010	0.010	7.767
	2	0.014	0.013	6.667	0.012	0.011	5.932	0.012	0.011	5.882	0.013	0.012	6.107
	3	0.013	0.012	7.031	0.013	0.012	7.087	0.014	0.013	6.993	0.014	0.013	5.185
	4	0.014	0.013	7.407	0.013	0.013	5.970	0.012	0.012	4.959	0.013	0.012	6.107
	5	0.012	0.011	5.217	0.013	0.012	5.344	0.012	0.012	6.504	0.012	0.011	6.667
	6	0.014	0.014	4.255	0.011	0.010	6.306	0.014	0.013	7.407	0.013	0.013	5.970

		7days			30days			60days			90days		
	No.	before	after	change	before	after	change	before	after	change	before	after	change
PLA/PEG/10% bone dECM	1	0.012	0.011	6.897	0.015	0.014	8.553	0.012	0.011	10.744	0.014	0.012	10.370
	2	0.015	0.014	7.534	0.016	0.015	6.962	0.013	0.011	10.236	0.017	0.015	9.091
	3	0.015	0.014	8.725	0.013	0.012	9.701	0.016	0.015	6.369	0.012	0.011	8.943
	4	0.011	0.010	7.547	0.014	0.013	7.692	0.016	0.015	7.547	0.015	0.014	9.868
	5	0.012	0.012	5.738	0.015	0.014	7.792	0.013	0.012	8.000	0.016	0.015	7.595
	6	0.013	0.012	7.200	0.016	0.015	7.362	0.015	0.013	9.655	0.015	0.013	9.655
PLA/PEG/20% bone	1	0.016	0.015	6.173	0.016	0.015	7.500	0.017	0.015	8.434	0.016	0.014	10.063
	2	0.015	0.014	8.725	0.016	0.014	9.677	0.016	0.014	8.917	0.018	0.016	10.286
	3	0.017	0.015	7.784	0.017	0.016	8.092	0.016	0.014	8.333	0.016	0.015	9.146
	4	0.016	0.015	8.537	0.017	0.016	8.671	0.015	0.014	8.442	0.015	0.014	9.211
	5	0.017	0.016	7.558	0.014	0.013	7.857	0.016	0.014	9.554	0.017	0.016	9.827
	6	0.015	0.014	6.494	0.016	0.014	8.333	0.016	0.015	10.366	0.013	0.012	9.023

Table A-2. The descriptive analysis of material degradation following the *in vitro* degration test in PBS at 7, 30, 60, and 90 days.

	N	Mean	Std. Deviation	Std. Error	95% Confidence Interval for Mean Lower Bound	95% Confidence Interval for Mean Upper Bound	Min	Max
PLA_7d	6	2.9452	1.00033	.40838	1.8954	3.9950	1.77	4.59
PLA_30d	6	3.5207	.85140	.34758	2.6272	4.4142	2.31	4.97
PLA_60d	6	4.1435	1.30973	.53469	2.7690	5.5180	2.86	6.45
PLA_90d	6	4.3195	.95701	.39070	3.3152	5.3238	3.01	5.31
PLA/PEG_7d	6	5.3205	1.28423	.52428	3.9728	6.6682	3.13	6.84
PLA/PEG _30d	6	5.5223	.69649	.28434	4.7914	6.2533	4.65	6.58
PLA/PEG _60d	6	5.8257	1.05922	.43243	4.7141	6.9373	4.69	7.38
PLA/PEG _90d	6	5.9072	1.01768	.41546	4.8392	6.9752	4.44	7.25
PLA/PEG/bone 5%_7d	6	6.1910	1.20420	.49161	4.9273	7.4547	4.26	7.41
PLA/PEG/bone 5%__30d	6	6.2403	.63393	.25880	5.5751	6.9056	5.34	7.09
PLA/PEG/bone 5%__60d	6	6.2500	.89469	.36526	5.3111	7.1889	4.96	7.41
PLA/PEG/bone 5%__90d	6	6.3005	.86179	.35182	5.3961	7.2049	5.19	7.77
PLA/PEG/bone 10%__7d	6	7.2735	.97513	.39810	6.2502	8.2968	5.74	8.73
PLA/PEG/bone 10%__30d	6	8.0103	.98196	.40088	6.9798	9.0408	6.96	9.70
PLA/PEG/bone 10%__60d	6	8.7585	1.71357	.69956	6.9602	10.5568	6.37	10.74
PLA/PEG/bone 10%__90d	6	9.2537	.96528	.39407	8.2407	10.2667	7.60	10.37
PLA/PEG/bone 20%__7d	6	7.5452	1.04122	.42508	6.4525	8.6379	6.17	8.73
PLA/PEG/bone 20%__30d	6	8.3550	.76108	.31071	7.5563	9.1537	7.50	9.68
PLA/PEG/bone 20%__60d	6	9.0077	.80697	.32944	8.1608	9.8545	8.33	10.37
PLA/PEG/bone 20%__90d	6	9.5927	.53414	.21806	9.0321	10.1532	9.02	10.29
Total	120	6.5141	2.10889	.19251	6.1329	6.8953	1.77	10.74

65

Table A-3. The statistical analysis by one-way ANOVA and Tukey multiple compariosn (α = 0.05) of material degradation following the *in vitro* degration test in PBS at 7, 30, 60, and 90 days.

Tests of Normality

	groups	Kolmogorov-Smirnov[a]			Shapiro-Wilk		
		Statistic	df	Sig.	Statistic	df	Sig.
Weight change	PLA_7d	.201	6	.200[*]	.952	6	.757
	PLA_30d	.294	6	.114	.898	6	.363
	PLA_60d	.213	6	.200[*]	.899	6	.369
	PLA_90d	.245	6	.200[*]	.898	6	.361
	blend_7d	.180	6	.200[*]	.944	6	.691
	blend_30d	.169	6	.200[*]	.979	6	.946
	blend_60d	.342	6	.027	.848	6	.153
	blend_90d	.186	6	.200[*]	.974	6	.918
	5_7d	.290	6	.126	.893	6	.334
	5_30d	.165	6	.200[*]	.968	6	.881
	5_60d	.160	6	.200[*]	.976	6	.930
	5_90d	.255	6	.200[*]	.927	6	.561
	10_7d	.223	6	.200[*]	.956	6	.792
	10_30d	.255	6	.200[*]	.918	6	.494
	10_60d	.200	6	.200[*]	.939	6	.655
	10_90d	.207	6	.200[*]	.941	6	.666
	20_7d	.177	6	.200[*]	.921	6	.512
	20_30d	.178	6	.200[*]	.939	6	.655
	20_60d	.258	6	.200[*]	.850	6	.157
	20_90d	.263	6	.200[*]	.885	6	.295

*. This is a lower bound of the true significance.
a. Lilliefors Significance Correction

66

Test of Homogeneity of Variances

Levene Statistic	df1	df2	Sig.
1.116	19	100	.347

One-way ANOVA

	Sum of Squares	df	Mean Square	F	Sig.
Between Groups	427.108	19	22.479	22.009	.000
Within Groups	102.135	100	1.021		
Total	529.243	119			

Table A-4. The statistical analysis by Tukey multiple compariosn ($\alpha = 0.05$) of material degradation following the *in vitro* degration test in PBS at 7, 30, 60, and 90 days.

Tukey HSD[a]

groups	N	Subset for alpha = 0.05									
		1	2	3	4	5	6	7	8	9	10
PLA_7d	6	2.9452									
PLA_30d	6	3.5207	3.5207								
PLA_60d	6	4.1435	4.1435	4.1435							
PLA_90d	6	4.3195	4.3195	4.3195	4.3195						
blend_7d	6		5.3205	5.3205	5.3205	5.3205					
blend_30d	6		5.5223	5.5223	5.5223	5.5223	5.5223				
blend_60d	6			5.8257	5.8257	5.8257	5.8257				
blend_90d	6			5.9072	5.9072	5.9072	5.9072	5.9072			
5_7d	6			6.1910	6.1910	6.1910	6.1910	6.1910			
5_30d	6			6.2403	6.2403	6.2403	6.2403	6.2403	6.2403		
5_60d	6			6.2500	6.2500	6.2500	6.2500	6.2500	6.2500		
5_90d	6				6.3005	6.3005	6.3005	6.3005	6.3005		
10_7d	6					7.2735	7.2735	7.2735	7.2735	7.2735	
20_7d	6						7.5452	7.5452	7.5452	7.5452	7.5452
10_30d	6							8.0103	8.0103	8.0103	8.0103
20_30d	6								8.3550	8.3550	8.3550
10_60d	6									8.7585	8.7585
20_60d	6									9.0077	9.0077
10_90d	6									9.2537	9.2537
20_90d	6										9.5927
Sig.		.692	.090	.055	.099	.112	.082	.056	.052	.099	.073

Means for groups in homogeneous subsets are displayed.
a. Uses Harmonic Mean Sample Size = 6.000.

Table A-5. Tha data of surface contact angles (degree) of each specimens.

Group	1	2	3	4
Pure PLA	69.9	69.435	69.5	68.88
PLA/PEG	56.76	56.485	55.57	54.82
PLA/PEG/bone dECM 5%	54.955	55.06	55.5	54.53
PLA/PEG/bone dECM 10%	56.465	57.01	55.425	56.375
PLA/PEG/bone dECM 20%	55.025	55.065	55	54.49

Table A-6. The descriptive analysis of the surface contact angle

	N	Mean	Std. Deviation	Std. Error	95% Confidence Interval for Mean Lower Bound	Upper Bound	Minimum	Maximum
Pure PLA	4	69.4288	.41965	.20983	68.7610	70.0965	68.88	69.90
PLA/PEG	4	55.9088	.88634	.44317	54.4984	57.3191	54.82	56.76
PLA/PEG/bone dECM 5%	4	55.0113	.39834	.19917	54.3774	55.6451	54.53	55.50
PLA/PEG/bone dECM 10%	4	56.1575	.41910	.20955	55.4906	56.8244	55.64	56.59
PLA/PEG/bone dECM 20%	4	54.8950	.27132	.13566	54.4633	55.3267	54.49	55.07
Total	20	58.2803	5.75998	1.28797	55.5845	60.9760	54.49	69.90

Table A-7. The statistical analysis by one-way ANOVA (α = 0.05) of surface contact angle.

Tests of Normality

	group	Kolmogorov-Smirnov[a]			Shapiro-Wilk		
		Statistic	df	Sig.	Statistic	df	Sig.
Angle	Pure PLA	.256	4	.	.959	4	.773
	PLA/PEG	.242	4	.	.936	4	.632
	PLA/PEG/bone dECM5%	.201	4	.	.983	4	.920
	PLA/PEG/bone dECM10%	.206	4	.	.969	4	.833
	PLA/PEG/bone dECM20%	.401	4	.	.722	4	.020

a. Lilliefors Significance Correction

Test of Homogeneity of Variances

Levene Statistic	df1	df2	Sig.
2.833	4	15	.062

One-way ANOVA

	Sum of Squares	df	Mean Square	F	Sig.
Between Groups	626.262	4	156.565	571.555	.000
Within Groups	4.109	15	.274		
Total	630.371	19			

70

Table A-8. The statistical analysis by Tukey multiple compariosn (α = 0.05) of surface contact angle.

Tukey HSD^a

group	N	Subset for alpha = 0.05		
		1	2	3
PLA/PEG/bone dECM20%	4	54.8950		
PLA/PEG/bone dECM5%	4	55.0113		
PLA/PEG	4	55.9088	55.9088	
PLA/PEG/bone dECM10%	4		56.1575	
Pure PLA	4			69.4288
Sig.		.094	.959	1.000

Means for groups in homogeneous subsets are displayed, a. Uses Harmonic Mean Sample Size = 4.000.

Table A- 9. The data of optical density and cell viability.

Optical density (OD)

		PLA	PLA/PEG	PLA/PEG/5%	PLA/PEG/10%	PLA/PEG/20%	control
1day	1	0.24121	0.26053	0.27737	0.31711	0.34277	0.43648
	2	0.23426	0.25036	0.2758	0.28991	0.28736	0.40212
	3	0.25914	0.23736	0.29484	0.29042	0.32173	0.48788
7days	1	0.99518	1.28744	1.26896	1.41097	1.64343	1.4555
	2	1.01004	1.22744	1.25921	1.39195	1.64928	1.40885
	3	0.96116	1.22726	1.26992	1.37887	1.69568	1.40328

% Cell viability

		PLA	PLA/PEG	PLA/PEG/5%	PLA/PEG/10%	PLA/PEG/20%	control
	1	54.6	58.92	62.73	71.72	77.52	98.72
1 day	2	53	56.62	62.38	65.57	64.99	90.94
	3	58.6	53.68	66.68	65.68	72.76	110.34
	1	225	291.17	286.99	319.11	371.68	329.18
7 days	2	228	277.60	284.79	314.81	373.01	318.63
	3	217	277.56	287.21	311.85	383.50	317.37

Table A-10. The descriptive analysis of the cell viability (%).

Descriptive

	N	Mean	Std. Deviation	Std. Error	95% Confidence Interval for Mean Lower Bound	Upper Bound	Min	Max
PLA_1 day	3	55.3804	2.90335	1.67625	48.1681	62.5927	52.98	58.61
PLA_7days	3	223.6279	5.66719	3.27195	209.5499	237.7060	217.38	228.43
PLA/PEG_7days	3	56.4067	2.62651	1.51641	49.8821	62.9313	53.68	58.92
PLA/PEG_7days	3	282.1100	7.84622	4.53001	262.6189	301.6011	277.56	291.17
PLA/PEG/bone 5%_1day	3	63.9300	2.38799	1.37871	57.9979	69.8621	62.38	66.68
PLA/PEG/bone 5%_7days	3	286.3300	1.33821	.77261	283.0057	289.6543	284.79	287.21
PLA/PEG/bone 10%_1day	3	67.6567	3.51938	2.03191	58.9140	76.3993	65.57	71.72
PLA/PEG/bone 10%_7days	3	315.2567	3.65055	2.10765	306.1882	324.3251	311.85	319.11
PLA/PEG/bone 20%_1day	3	71.7567	6.32497	3.65172	56.0446	87.4688	64.99	77.52
PLA/PEG/bone 20%_7days	3	376.0633	6.47458	3.73810	359.9796	392.1471	371.68	383.50
Control_1d	3	100.0000	9.76313	5.63675	75.7470	124.2530	90.94	110.34
Control_7days	3	321.7267	6.48545	3.74438	305.6159	337.8374	317.37	329.18
Total	36	185.0204	122.61835	20.43639	143.5323	226.5085	52.98	383.50

Table A-11. The statistical analysis by one-way ANOVA (α=0.05) of cell viability (%).

Tests of Normality

	group	Kolmogorov-Smirnov[a]			Shapiro-Wilk		
		Statistic	df	Sig.	Statistic	df	Sig.
viability	PLA_1 day	.279	3	.	.939	3	.524
	PLA_7days	.267	3	.	.951	3	.575
	PLA/PEG_1days	.199	3	.	.995	3	.866
	PLA/PEG_7days	.384	3	.	.752	3	.005
	PLA/PEG/bone 5%_1day	.359	3	.	.811	3	.140
	PLA/PEG/bone 5%_7days	.356	3	.	.818	3	.157
	PLA/PEG/bone 10%_1day	.379	3	.	.763	3	.030
	PLA/PEG/bone 10%_7days	.215	3	.	.989	3	.797
	PLA/PEG/bone 20%_1day	.230	3	.	.981	3	.737
	PLA/PEG/bone 20%_7 days	.348	3	.	.833	3	.197
	Control_1d	.219	3	.	.987	3	.783
	Control_7days	.350	3	.	.829	3	.186

a. Lilliefors Significance Correction

Test of Homogeneity of Variances

Levene Statistic	df1	df2	Sig.
1.921	11	24	.088

74

One-way ANOVA

	Sum of Squares	df	Mean Square	F	Sig.
Between Groups	525511.057	11	47773.732	1585.765	.000
Within Groups	723.039	24	30.127		
Total	526234.095	35			

Table A-12. The statistical analysis by Tukey multiple compariosn (α = 0.05) of cell viability (%).

Tukey HSD[a]

group	N	1	2	3	4	5	6	7
		Subset for alpha = 0.05
PLA_1 day	3	55.3804						
PLA/PEG_1days	3	56.4067	56.4067					
PLA/PEG/bone 5%_1day	3	63.9300	63.9300					
PLA/PEG/bone 10%_1day	3	67.6567	67.6567					
PLA/PEG/bone 20%_1day	3		71.7567					
Control_1d	3			100.0000				
PLA_7days	3				223.6279			
PLA/PEG_7days	3					282.1100		
PLA/PEG/bone 5%_7days	3					286.3300		
PLA/PEG/bone 10%_7days	3						315.2567	
Control_7days	3						321.7267	
PLA/PEG/bone 20%_7 days	3							376.0633
Sig.		.266	.073	1.000	1.000	.998	.942	1.000

Means for groups in homogeneous subsets are displayed.

a. Uses Harmonic Mean Sample Size = 3.000.

75

Table A-13. The optical density value (at 568 nm) of Alizarin Red S staining following the incubation toward the MG-63 cells for 14A days and the result of the statistical analysis (one-way ANOVA , α=0.05).

Optical density (OD) at 568 nm

	complete medium (Negative control)	Complete medium with extraction	Osteogenic medium (Positive control)
1	0.0868	0.1908	0.2419
2	0.0972	0.193	0.2456
3	0.0935	0.1818	0.2465

Table A-14. The descriptive data of the OD of Alizarin Red S staining.

Descriptive

	N	Mean	Std. Deviation	Std. Error	95% Confidence Interval for Mean Lower Bound	95% Confidence Interval for Mean Upper Bound	Min.	Max.
Complete medium	3	.0925	.00527	.00304	.0794	.1056	.09	.10
Complete medium with material extraction	3	.1885	.00593	.00343	.1738	.2033	.18	.19
Osteogenic medium	3	.2447	.00244	.00141	.2386	.2507	.24	.25
Total	9	.1752	.06677	.02226	.1239	.2266	.09	.25

Table A-15. The statistical analysis by one-way ANOVA of the OD value of Alizarin Red S staining.

Tests of Normality

	group	Kolmogorov-Smirnov[a]			Shapiro-Wilk		
		Statistic	df	Sig.	Statistic	df	Sig.
OD	complete medium	.242	3	.	.973	3	.685
	complete medium with material extraction	.315	3	.	.891	3	.356
	osteogenic medium	.316	3	.	.890	3	.355

a. Lilliefors Significance Correction

Test of Homogeneity of Variances

Levene Statistic	df1	df2	Sig.
1.416	2	6	.313

One-way ANOVA

	Sum of Squares	df	Mean Square	F	Sig.
Between Groups	.036	2	.018	772.946	.000
Within Groups	.000	6	.000		
Total	.036	8			

Table A-16. The statistical analysis by Tukey multiple compariosn (α = 0.05) of the OD value of Alizarin Red S staining.

Tukey HSD[a]

group	N	Subset for alpha = 0.05		
		1	2	3
Complete medium	3	.0925		
Complete medium with material extraction	3		.1885	
Osteogenic medium	3			.2447
Sig.		1.000	1.000	1.000

Means for groups in homogeneous subsets are displayed.
a. Uses Harmonic Mean Sample Size = 3.000.

Appendix B

(Raw data and statistical analysis for second publication)

Table B-1. The data of dried weight, volume, and porosity of each scaffold.

N0.	Pristine PLA/PBAT scaffold			PLA/PBAT with PDA			PLA/PBAT with PDA-assisted biomineralization		
	Dried weight (g)	Vol. (cm^3)	Porosity (%)	Dried weight (g)	Vol. (cm^3)	Porosity (%)	Dried weight (g)	Vol. (cm^3)	Porosity (%)
1	0.05	0.49	87.74	0.04	0.40	86.64	0.06	0.44	84.70
2	0.04	0.36	85.40	0.04	0.31	85.49	0.05	0.33	81.96
3	0.05	0.50	87.63	0.05	0.55	87.65	0.06	0.51	85.35
4	0.03	0.32	86.56	0.04	0.37	85.37	0.04	0.34	84.53
5	0.05	0.46	86.59	0.05	0.51	89.04	0.04	0.34	84.28

Table B-2. The descriptive statistic of scaffold porosity (%).

	N	Mean	Std. Deviation	Std. Error	95% Confidence Interval for Mean		Minimum	Maximum
					Lower Bound	Upper Bound		
pristine PLA/PBAT scaffold	5	86.7831	.94969	.42471	85.6040	87.9623	85.40	87.74
PLA/PBAT with PDA	5	86.8388	1.54440	.69067	84.9212	88.7564	85.37	89.04
PLA/PBAT with PDA-assisted biomineralization	5	84.1650	1.29338	.57842	82.5591	85.7710	81.96	85.35
Total	15	85.9290	1.75630	.45348	84.9564	86.9016	81.96	89.04

Table B-3. The statistical analysis of scaffold porosity by one-way ANOVA and Tukey multiple comparison test (α=0.05).

Tests of Normality

	group	Kolmogorov-Smirnov[a]			Shapiro-Wilk		
		Statistic	df	Sig.	Statistic	df	Sig.
porosity	pristine PLA/PBAT scaffold	.212	5	.200[*]	.905	5	.439
	PLA/PBAT with PDA	.208	5	.200[*]	.921	5	.538
	PLA/PBAT with PDA-assisted biomineralization	.335	5	.069	.827	5	.132

*. This is a lower bound of the true significance.
a. Lilliefors Significance Correction

Test of homogeneity of variances

Levene Statistic	df1	df2	Sig.
.614	2	12	.557

One-way ANOVA

	Sum of Squares	df	Mean Square	F	Sig.
Between Groups	23.345	2	11.672	7.060	.009
Within Groups	19.840	12	1.653		
Total	43.184	14			

Table B-3. The statistical analysis of scaffold porosity by one-way ANOVA and Tukey multiple comparison test (α=0.05).

Tukey HSDa

		Subset for alpha = 0.05	
group	N	1	2
PLA/PBAT with PDA-assisted biomineralization	5	84.1650	
pristine PLA/PBAT scaffold	5		86.7831
PLA/PBAT with PDA	5		86.8388
Sig.		1.000	.997

Means for groups in homogeneous subsets are displayed, a. Uses Harmonic Mean Sample Size = 5.000.

Table B-4. The data of the compressive strength and modulus of elasticity of each scaffold.

No.	Pristine PLA/PBAT		PLA/PBAT with PDA-assisted biomineralization	
	Compressive strength (MPa)	Modulus of elasticity	Compressive strength (MPa)	Modulus of elasticity
1	0.96	0.058	0.84	0.040
2	1.17	0.096	0.42	0.060
3	0.93	0.068	0.65	0.070
4	1.1	0.094	0.49	0.050
5	1.2	0.067	0.87	0.030
Mean	1.07	0.65	0.08	0.05
SD	0.12	0.20	0.02	0.02

Table B-5. The descriptive statistic of compressive strength and modulus of elasticity.

	group	N	Mean	Std. Deviation	Std. Error Mean
compressive	PLA/PBAT with PDA-assisted biomineralization	5	.6540	.20182	.09026
	Pristine PLA/PBAT	5	1.0720	.12194	.05453

	group	N	Mean	Std. Deviation	Std. Error Mean
Modulus of elasticity	PLA/PBAT with PDA-assisted biomineralization	5	.0500	.01581	.00707
	Pristine PLA/PBAT	5	.0678	.01599	.00715

81

Table B-6. The statistical analysis of compressive strength by independent t-test (α=0.05).

Tests of Normality

	group	Kolmogorov-Smirnov[a]			Shapiro-Wilk		
		Statistic	df	Sig.	Statistic	df	Sig.
compressive	Pristine PLA/PBAT	.221	5	.200[*]	.890	5	.359
	PLA/PBAT with PDA-assisted biomineralization	.222	5	.200[*]	.903	5	.427

*. This is a lower bound of the true significance.

a. Lilliefors Significance Correction

Independent t-test

		Levene 's Test		t-test for Equality of Means					95% Confidence Interval of the Difference	
		F	Sig.	t	df	Sig. (2-tailed)	Mean Difference	Std. Error Difference	Lower	Upper
Compressive strength	Equal variances assumed	1.689	.230	-3.964	8	.004	-.41800	.10545	-.66117	-.17483
	Equal variances not assumed			-3.964	6.577	.006	-.41800	.10545	-.67064	-.16536

82

Table B-7. The statistical analysis of modulus of elasticity by independent t-test (α=0.05).

Tests of Normality

group		Kolmogorov-Smirnov[a]			Shapiro-Wilk		
		Statistic	df	Sig.	Statistic	df	Sig.
modulus	Pristine PLA/PBAT	.291	5	.193	.847	5	.187
	PLA/PBAT with PDA-assisted biomineralization	.136	5	.200[*]	.987	5	.967

*. This is a lower bound of the true significance.

a. Lilliefors Significance Correction

Independent Samples Test

		Levene 's Test		t-test for Equality of Means					95% Confidence Interval of the Difference	
		F	Sig.	t	df	Sig. (2-tailed)	Mean Difference	Std. Error Difference	Lower	Upper
modulus	Equal variances assumed	.382	.554	-2.541	8	.035	-.02660	.01047	-.05074	-.00246
	Equal variances not assumed			-2.541	7.940	.035	-.02660	.01047	-.05077	-.00243

83

Table B-8. The data of the ontact angles (degree) of each specimen.

N0.	Pristine scaffold	Scaffold with PDA	scaffold with PDA-assisted biomineralization
1	71	54	45
2	73	61	44
3	67	44	53
4	67	45	45
5	70	56	40
6	73	61	40
7	71	58	56
8	74	53	52
9	68	48	40
10	70	53	42

Table B-9. The descriptive analysis of surface contact angle**.**

	N	Mean	Std. Deviation	Std. Error	95% Confidence Interval for Mean		Minimum	Maximum
					Lower Bound	Upper Bound		
pristine PLA/PBAT	10	70.4000	2.50333	.79162	68.6092	72.1908	67.00	74.00
PLA/PBAT with PDA	10	53.3000	6.07454	1.92094	48.9545	57.6455	44.00	61.00
PLA/PBAT with PDA-assisted biomineralization	10	45.7000	5.90762	1.86815	41.4739	49.9261	40.00	56.00
Total	30	56.4667	11.60182	2.11819	52.1345	60.7989	40.00	74.00

84

Table B-10. The statistical analysis of surface contact angle by one-way ANOVA (α=0.05).

Tests of Normality

	group	Kolmogorov-Smirnov[a]			Shapiro-Wilk		
		Statistic	df	Sig.	Statistic	df	Sig.
Contact Angle	pristine PLA/PBAT	.151	10	.200*	.925	10	.404
	PLA/PBAT with PDA	.180	10	.200*	.929	10	.442
	PLA/PBAT with PDA-assisted biomineralization	.247	10	.084	.860	10	.077

*. This is a lower bound of the true significance.
a. Lilliefors Significance Correction

Test of homogeneity of variances

Levene Statistic	df1	df2	Sig.
3.171	2	27	.058

One-way ANOVA

	Sum of Squares	df	Mean Square	F	Sig.
Between Groups	3200.867	2	1600.433	61.503	.000
Within Groups	702.600	27	26.022		
Total	3903.467	29			

Table B- 11. The multiple comparison of surface contact angle by Tukey test (α=0.05).

Tukey HSD[a]

group	N	Subset for alpha = 0.05		
		1	2	3
PLA/PBAT with PDA-assisted biomineralization	10	45.7000		
PLA/PBAT with PDA	10		53.3000	
pristine PLA/PBAT	10			70.4000
Sig.		1.000	1.000	1.000

Means for groups in homogeneous subsets are displayed.
a. Uses Harmonic Mean Sample Size = 10.000.

Table B-12. The data of the percentage of water uptake at each investing period.

No.	24h		7 days		15 days		30 days	
	PLA/PBAT	PLA/PBAT with PDA-HA	PLA/PBAT	PLA/PBAT with PDA-HA	PLA/PBAT	PLA/PBAT with PDA-HA	PLA/PBAT	PLA/PBAT with PDA-HA
1	342.63	372.22	596.26	571.38	720.53	721.05	716.53	686.46
2	267.26	381.61	686.04	655.11	661.68	678.83	726.65	683.28
3	256.54	377.72	683.88	641.81	739.45	763.68	705.53	650.15
4	329.28	420.49	657.50	598.98	695.30	699.70	673.64	723.81
5	335.76	394.61	653.52	641.74	729.21	721.65	679.25	727.96

Table B-13. The descriptive statistic of the percentage of water uptake at each investigating period.

	N	Mean	Std. Deviation	Std. Error	95% Confidence Interval for Mean		Min	Max
					Lower Bound	Upper Bound		
Pristine_24h	5	306.2940	40.97566	18.32487	255.4160	357.1720	256.54	342.63
Modify_24	5	389.3300	19.27412	8.61965	365.3980	413.2620	372.22	420.49
Pristine_7	5	655.4400	36.24706	16.21018	610.4333	700.4467	596.26	686.04
Modify_7	5	621.8040	35.25085	15.76466	578.0343	665.5737	571.38	655.11
Pristine_15	5	709.2340	31.20571	13.95562	670.4870	747.9810	661.68	739.45
Modify_15	5	716.9820	31.51700	14.09483	677.8485	756.1155	678.83	763.68
Pristine_30	5	700.3200	23.12436	10.34153	671.6073	729.0327	673.64	726.65
Modify_30	5	694.3320	32.15571	14.38047	654.4054	734.2586	650.15	727.96
Total	40	599.2170	154.12403	24.36915	549.9257	648.5083	256.54	763.68

86

Table B-14. The statistical analysis of the percentage of water uptake (1-way ANOV, α=.05).

Tests of Normality

	group	Kolmogorov-Smirnov[a]			Shapiro-Wilk		
		Statistic	df	Sig.	Statistic	df	Sig.
Water Uptake	P24	.313	5	.124	.810	5	.097
	Min24	.256	5	.200*	.880	5	.309
	P7	.279	5	.200*	.854	5	.208
	Min7	.314	5	.120	.876	5	.292
	P15	.241	5	.200*	.920	5	.532
	Min15	.241	5	.200*	.958	5	.793
	P30	.219	5	.200*	.915	5	.496
	Min30	.220	5	.200*	.914	5	.495

*. This is a lower bound of the true significance.

a. Lilliefors Significance Correction

Test of homogeneity of variances

Levene Statistic	df1	df2	Sig.
.855	7	32	.552

One-way ANOVA

	Sum of Squares	df	Mean Square	F	Sig.
Between Groups	893843.252	7	127691.893	125.452	.000
Within Groups	32571.245	32	1017.851		
Total	926414.497	39			

87

Table B-15. The statistical analysis of the percentage of water uptake by Tukey multiple comparison (α=.05).

Tukey HSD[a]

group	N	Subset for alpha = 0.05			
		1	2	3	4
P24	5	306.2940			
Min24	5		389.3300		
Min7	5			621.8040	
P7	5			655.4400	655.4400
Min30	5				694.3320
P30	5				700.3200
P15	5				709.2340
Min15	5				716.9820
Sig.		1.000	1.000	.707	.077

Means for groups in homogeneous subsets are displayed.

a. Uses Harmonic Mean Sample Size = 5.000.

Table B-16. The percentage of material weight change following the *in vitro* degradation test for 7, 15, and 30 days.

	Pristine PLA/PBAT				PLA/PBAT with PDA-assisted biomineralization			
	initial	after	Weight change	Weight change	initial	after	Weight change	Weight change
	(g)	(g)	(g)	(%)	(g)	(g)	(g)	(%)
7 days	0.029	0.028	0.001	3.401	0.028	0.027	0.001	2.500
	0.039	0.039	0.000	1.015	0.037	0.036	0.001	3.495
	0.027	0.027	0.000	1.465	0.040	0.037	0.003	6.801
	0.024	0.024	0.000	0.833	0.036	0.035	0.001	3.047
	0.021	0.021	0.001	3.756	0.033	0.032	0.002	5.405
15 days	0.019	0.017	0.002	9.424	0.035	0.033	0.002	4.611
	0.019	0.017	0.002	11.518	0.029	0.027	0.001	4.530
	0.019	0.018	0.001	4.663	0.029	0.026	0.003	9.123
	0.024	0.022	0.002	7.203	0.029	0.026	0.003	11.419
	0.019	0.018	0.001	6.186	0.027	0.025	0.002	5.618
30 days	0.036	0.033	0.003	7.263	0.025	0.024	0.002	6.324
	0.034	0.033	0.002	4.971	0.031	0.028	0.003	9.740
	0.022	0.020	0.002	10.046	0.033	0.032	0.002	4.790
	0.020	0.018	0.002	10.000	0.031	0.028	0.003	10.897
	0.032	0.029	0.003	8.696	0.027	0.025	0.002	6.415

89

Table B-17. The descriptive statistic of material weight change following the in vitro degradation test for 7, 15, and 30 days.

	N	Mean	SD	Std. Error	95% Confidence Interval for Mean		Min.	Max.
					Lower Bound	Upper Bound		
Pristine 7 days	5	2.0940	1.38026	.61727	.3802	3.8078	.83	3.76
Biomineralization 7 days	5	4.2496	1.79731	.80378	2.0179	6.4813	2.50	6.80
Pristine 15 days	5	7.7988	2.70477	1.20961	4.4404	11.1572	4.66	11.52
Biomineralization 15 days	5	7.0602	3.07143	1.37358	3.2465	10.8739	4.53	11.42
Pristine 30 days	5	8.1952	2.13296	.95389	5.5468	10.8436	4.97	10.05
Biomineralization 30 days	5	7.6332	2.56772	1.14832	4.4450	10.8214	4.79	10.90
Total	30	6.1718	3.11868	.56939	5.0073	7.3364	.83	11.52

Table B-18. The statistical analysis of material weight change by one-way ANOVA ($\alpha=0.05$).

Tests of Normality

	Kolmogorov-Smirnov[a]			Shapiro-Wilk		
group	Statistic	df	Sig.	Statistic	df	Sig.
Pristine 7d	.276	5	.200[*]	.832	5	.145
Biomineralization 7d	.263	5	.200[*]	.909	5	.463
Pristine 15d	.187	5	.200[*]	.974	5	.898
Biomineralization 15d	.281	5	.200[*]	.851	5	.199
Pristine 30d	.201	5	.200[*]	.894	5	.378
Biomineralization 30d	.282	5	.200[*]	.904	5	.434

*. This is a lower bound of the true significance, a. Lilliefors Significance Correction

Test of homogeneity of variances

Levene Statistic	df1	df2	Sig.
1.458	5	24	.240

One-way ANOVA

	Sum of Squares	df	Mean Square	F	Sig.
Between Groups	149.948	5	29.990	5.448	.002
Within Groups	132.110	24	5.505		
Total	282.058	29			

90

Table B-19. The statistical analysis of material wight change (%) by Tukey multiple comparison (α=0.05).

Tukey HSD[a]

| group | N | Subset for alpha = 0.05 | |
		1	2
Pristine 7d	5	2.0940	
Biomineralization 7d	5	4.2496	4.2496
Pristine 15d	5		7.0602
Biomineralization 15d	5		7.6332
Pristine 30d	5		7.7988
Biomineralization 30d	5		8.1952
Sig.		.696	.121

Means for groups in homogeneous subsets are displayed, a. Uses Harmonic Mean Sample Size = 5.000.

Table B-20. The pH alteration data of soaking medium at various investigating period

	No.	Pristine PLA/PBAT	No.	PLA/PBAT with PDA-assisted biomineralization
0 day	1	7.33	1	7.33
	2	7.3	2	7.31
	3	7.32	3	7.33
	4	7.33	4	7.29
	5	7.31	5	7.30
7 days	1	7.29	1	7.26
	2	7.28	2	7.25
	3	7.29	3	7.27
	4	7.31	4	7.27
	5	7.29	5	7.28
15 days	1	7.25	1	7.25
	2	7.28	2	7.26
	3	7.29	3	7.27
	4	7.28	4	7.27
	5	7.28	5	7.25
30 days	1	7.28	1	7.25
	2	7.24	2	7.25
	3	7.28	3	7.25
	4	7.28	4	7.24
	5	7.28	5	7.24

Table B-21. The statistical analysis of the pH alteration data by one-way ANOVA (α=0.05).

Tests of Normality

	group	Kolmogorov-Smirnov[a]			Shapiro-Wilk		
		Statistic	df	Sig.	Statistic	df	Sig.
pH Change	p7d	.141	5	.200[*]	.979	5	.928
	Min7d	.237	5	.200[*]	.961	5	.814
	p15d	.310	5	.131	.871	5	.272
	Min15d	.241	5	.200[*]	.821	5	.119
	p30d	.258	5	.200[*]	.782	5	.057
	Min30d	.213	5	.200[*]	.963	5	.826
	p0d	.221	5	.200[*]	.902	5	.421
	Min0d	.243	5	.200[*]	.894	5	.377

*. This is a lower bound of the true significance, a. Lilliefors Significance Correction

Test of homogeneity of variances

Levene Statistic	df1	df2	Sig.
1.275	7	32	.294

One-way ANOVA

	Sum of Squares	df	Mean Square	F	Sig.
Between Groups	.024	7	.003	11.724	.000
Within Groups	.009	32	.000		
Total	.033	39			

92

Table B-22. The statistical analysis of the pH alteration data by Tukey multiple comparison (α=0.05).

Tukey HSD^a

group	N	Subset for alpha = 0.05			
		1	2	3	4
Min30d	5	7.2460			
p30d	5	7.2580	7.2580		
Min15d	5	7.2600	7.2600		
Min7d	5	7.2660	7.2660		
p15d	5	7.2680	7.2680		
p7d	5		7.2820	7.2820	
Min0d	5			7.3120	7.3120
p0d	5				7.3180
Sig.		.468	.360	.133	.999

Means for groups in homogeneous subsets are displayed.

a. Uses Harmonic Mean Sample Size = 5.000.

Table B-23. The optical density (OD) of MTT assay and the calculated percentage of cell viability.

Optical density (OD value)

		Control	Pristine PLA/PBAT	PLA/PBAT with PDA-assisted biomineralization	TritonX-100 (Negative control)
1 d	1	0.3949	0.3486	0.3649	0.0036
	2	0.3812	0.3478	0.3408	0.0054
	3	0.3942	0.3732	0.3445	0.0082
3 d	1	0.9407	1.0452	1.1135	0.0324
	2	0.8427	0.8256	0.9637	0.0405
	3	1.0559	0.8469	0.8503	O0.0380
5 d	1	1.9886	1.8685	1.5364	0.0110
	2	1.7163	1.8527	1.5239	0.0191
	3	1.8439	1.7812	1.4413	0.0166

Cell viability (%)

		Control	Pristine PLA/PBAT	PLA/PBAT with PDA-assisted biomineralization	TritonX-100 (Negative control)
1 d	1	101.23	89.36	93.54	0.92
	2	97.72	89.16	87.36	1.38
	3	101.05	95.67	88.31	2.10
3 d	1	245.48	272.74	290.57	8.46
	2	219.91	215.45	251.48	10.58
	3	275.54	221.01	221.89	9.92
5 d	1	509.80	479.01	393.87	2.83
	2	439.99	474.96	390.67	4.90
	3	101.23	89.36	93.54	0.92

Table B-24. The descriptive statistic of the calculated percentage of cell viability values.

Descriptive

	N	Mean	Std. Deviation	Std. Error	95% Confidence Interval for Mean		Min	Max
					Lower Bound	Upper Bound		
pristine_1d	3	91.395	3.702	2.137	82.200	100.590	89.160	95.670
HA_1d	3	89.737	3.327	1.921	81.472	98.002	87.360	93.540
Pristine_3d	3	236.400	31.598	18.243	157.907	314.892	215.450	272.740
HA_3d	3	254.646	34.446	19.887	169.077	340.214	221.890	290.570
Pristine_5d	3	470.199	11.925	6.885	440.575	499.822	456.630	479.010
HA_5d	3	384.679	13.248	7.649	351.770	417.588	369.490	393.870
Control_1d	3	100.000	1.978	1.142	95.087	104.913	97.720	101.230
Control_3d	3	246.977	27.843	16.075	177.811	316.142	219.910	275.540
Control_5d	3	474.164	34.926	20.164	387.403	560.924	439.990	509.800
TritonX_1d	3	1.466	0.594	0.343	-0.011	2.942	0.920	2.100
TritonX_3d	3	9.655	1.082	0.625	6.966	12.344	8.460	10.580
TritonX_5d	3	3.999	1.063	0.614	1.358	6.641	2.830	4.900
Total	36	196.943	170.643	28.440	139.206	254.680	0.920	509.800

Table B-25. The statistical analysis of the calculated percentage of cell viability by one-way ANOVA (α=0.065).

Tests of Normality

	Group	Kolmogorov-Smirnov[a]			Shapiro-Wilk		
		Statistic	df	Sig.	Statistic	df	Sig.
Cell	pristine_1d	.375	3	.	.774	3	.053
Viability	HA_1d	.333	3	.	.862	3	.273
	Pristine_3d	.354	3	.	.822	3	.168
	HA_3d	.203	3	.	.994	3	.848
	Pristine_5d	.322	3	.	.881	3	.326
	HA_5d	.341	3	.	.847	3	.232
	Control_1d	.369	3	.	.788	3	.087
	Control_3d	.188	3	.	.998	3	.911
	Control_5d	.183	3	.	.999	3	.931
	TritonX_1d	.224	3	.	.984	3	.762
	TritonX_3d	.265	3	.	.953	3	.585
	TritonX_5d	.265	3	.	.953	3	.585

Means for groups in homogeneous subsets are displayed., a. Lilliefors Significance Correction

Test of homogeneity of variances

Levene Statistic	df1	df2	Sig.
3.318	11	24	.007

One-way ANOVA

	Sum of Squares	df	Mean Square	F	Sig.
Between Groups	1010103.805	11	91827.619	243.305	.000
Within Groups	9058.032	24	377.418		
Total	1019161.836	35			

Table B-26. The statistical analysis of the percentage of cell viability by Tukey multiple comparison (α=0.05).

Tukey HSD[a]

Group	N	1	2	3	4	5
		Subset for alpha = 0.05				
TritonX_1d	3	1.4655				
TritonX_5d	3	3.9991				
TritonX_3d	3	9.6551				
HA_1d	3		89.7372			
pristine_1d	3		91.3950			
Control_1d	3		100.0000			
Pristine_3d	3			236.3995		
Control_3d	3			246.9766		
HA_3d	3			254.6456		
HA_5d	3				384.6785	
Pristine_5d	3					470.1987
Control_5d	3					474.1636
Sig.		1.000	1.000	.988	1.000	1.000

Means for groups in homogeneous subsets are displayed.

a. Uses Harmonic Mean Sample Size = 3.000.

Table B-27. The optical density at 570 nm of Alizarin Red S staining following the incubation for 21 days.

OD (570 nm)

No.	General Medium	Pristine PLA/PBAT extraction medium	PLA/PBAT with PDA-assisted biomineralization extraction medium	Osteogenic medium
1	1.005775	0.873686	1.677477	2.431512
2	0.930549	0.889679	1.526433	2.312454
3	0.959574	0.825115	1.620021	2.414334
4	1.104102	0.957204	1.724271	2.266252

Table B-28. The descriptive statistic of the optical density values.

Descriptive

	N	Mean	Std. Deviation	Std. Error	Lower Bound	Upper Bound	Minimum	Maximum
					95% Confidence Interval for Mean			
General medium	4	1.0000	.07600	.03800	.8791	1.1209	.93	1.10
Pristine scaffold	4	.8864	.05459	.02730	.7996	.9733	.83	.96
Scaffold with PDA-assisted biomineralization	4	1.6371	.08518	.04259	1.5015	1.7726	1.53	1.72
Osteogenic medium	4	2.3561	.07970	.03985	2.2293	2.4830	2.27	2.43
Total	16	1.4699	.60913	.15228	1.1453	1.7945	.83	2.43

Table B-29. The statistical analysis of the optical density value **(α=0.05).**

Test of Normality

	group	Statistic	df	Sig.	Statistic	df	Sig.
		Kolmogorov-Smirnov[a]			Shapiro-Wilk		
OD (570 nm)	General medium	.220	4	.	.930	4	.596
	Pristine scaffold	.226	4	.	.976	4	.881
	Scaffold with PDA-assisted biomineralization	.182	4	.	.973	4	.859
	Osteogenic Medium	.267	4	.	.894	4	.402

a. Lilliefors Significance Correction

Test of homogeneity of variances

Levene Statistic	df1	df2	Sig.
.559	3	12	.652

One-way ANOVA

	Sum of Squares	df	Mean Square	F	Sig.
Between Groups	5.498	3	1.833	327.808	.000
Within Groups	.067	12	.006		
Total	5.566	15			

Table B-30. The statistical analysis of the optical density values by Tukey multiple comparison (α=0.05).

Tukey HSD[a]

		Subset for alpha = 0.05		
group	N	1	2	3
Pristine scaffold	4	.8864		
General medium	4	1.0000		
Scaffold with PDA-assisted biomineralization	4		1.6371	
Osteogenic medium	4			2.3561
Sig.		.193	1.000	1.000

Means for groups in homogeneous subsets are displayed.

a. Uses Harmonic Mean Sample Size = 4.000.

99

CURRICULUM VITAE

Author's Name   Mr. Kullapop Suttiat

Education   2000   Doctor of Dental Surgery (D.D.S.), Faculty of Dentistry,
                              Chiang Mai University.

                       2003   Graduate Diploma Program in Clinical Science
                              (Prosthodontics), Faculty of Dentistry, Chiang Mai
                              University.

                       2010   Master of Science (M.Sc.) Prosthodontics, Faculty of
                              Dentistry, Chulalongkorn University.

                       2014   Fellowship of the Royal College of Dental Surgeon of
                              Thailand, The Royal College of Dental Surgeon of
                              Thailand.

Scholarship   The National Research Council of Thailand (NRTC), Grant No.
                       2934737 (During 2021 to 2022).

Publications   Suttiat, K., Wattanutchariya, W., & Manaspon, C. (2022).
                       Preparation and Characterization of Porous Poly (Lactic
                       Acid)/Poly (Butylene Adipate-Co-Terephthalate) (PLA/PBAT)
                       Scaffold with Polydopamine-Assisted Biomineralization for
                       Bone Regeneration. Materials, 15(21), 7756.

                       Wattanutchariya, W., & Suttiat, K. (2022). Characterization of
                       Polylactic/Polyethylene glycol/Bone Decellularized
                       Extracellular Matrix Biodegradable Composite for Tissue
                       Regeneration. CMU Journal of Natural Science, 21(1),
                       e2022008.

100

Publications   Rungsiyakull, C., Rungsiyakull, P., Suttiat, K., & Duangrattanaprathip, N. (2022). Stress distribution pattern in mini dental implant-assisted RPD with different clasp designs: 3D finite element analysis. International Journal of Dentistry, 2022.

Boonpok, S., Koonrungsrisomboon, K., Suttiat, K., Yavirach, P., & Boonyawan, D. (2022). Dissolution Behavior of Hydrothermally Treated Hydroxyapatite–Titanium Nitride Films Coated on PEEK: In Vitro Study. Journal of Functional Biomaterials, 13(3), 99.

Koonrungsesomboon, K., Boonyawan, D., Suttiat, K., & Yavirach, P. (2022). Effect of immersion time in simulated body fluid on adhesion strength of hydrothermally treated hydroxyapatite-titanium nitride films on polyetheretherketones.

101